EVOLUTION OF H_2S AND SO_2 DURING RAPID HEATING OF
PULVERIZED COAL AND SULFUR CONTAINING MODEL COMPOUNDS

by

JAYARAM POLAVARAPU

M.Sc., Andhra University, Waltair, India, 1975

LD
2668
.T4
1979
P63
c.2

TABLE OF CONTENTS

LIST OF TABLES

LIST OF FIGURES

iv

NOMENCLATURE

C	concentration (ppm)
E	activation energy (kcal/mole)
k	reaction rate constant
M_s	shock Mach number
Mw	molecular weight (gm)
n_{TG}	total number of moles of test gas
P	pressure (torr)
R	universal gas constant; 1.987 cal/mole K; 82.05 atm cm^3/ mole K
T	temperature (K)
t	time (sec)
V	volume (cm^3)
W	weight (gm)
x	H_2S or SO_2 concentration (ppm)
y	difference in the maximum yield of H_2S or SO_2 and the yield at a particular temperature (ppm)

Greek Symbols

γ	gas specific heat ratio

1.0 Introduction

Political and economic pressures have required and will continue
to require an increased use of "dirty coal" (i.e., high sulfur con-
tent) for the production of electricity. Thus a significant amount of
research on the combustion of coal is in the areas of pollution formation
and control. The sulfurous products of coal combustion are primarily
SO_2, H_2S, and small amounts of SO_3.

SO_2 emissions from combustion sources, unless checked in the near
future, will be increasing to serious proportions. Emissions are esti-
mated currently at 22 million tons per year with forecast of 42 million
tons by 1980 (1). Essentially all of the sulfur from coal or oil will
be leaving the stacks as SO_2, with small amounts of SO_3. Solution to
this problem could be either removal of sulfur before combustion and/or
removal of SO_2 from the stack gas after combustion. A significant
portion of the iron pyrites can be removed prior to combustion, but
not the organically bound sulfur. Since pyritic sulfur in coal occurs
in finely disseminated particles, these particles can be removed
mechanically by froth flotation and gravity concentration. In mechanical
cleaning, screens of different pore sizes are used, separating particles
by size. In froth-flotation, the coal feed is agitated in a controlled
amount of water, air and reagents. The reagents used are aqueous
solution of salts such as calcium chloride and zinc chloride and organic
liquids such as carbon tetrachloride, bromoform, ethylene dibromide and
naphta. As the result of agitation, a surface froth is formed.

The bubbles selectively attach themselves to coal particles and keep them buoyant while the heavier particles of pyrite remain dispersed in the water. In gravity concentration the heavier particles separate from lighter ones when settling in a fluid. Iron pyrite has a specific gravity of 5 while coals have a specific gravity of 1.25. The commercial process used in gravity concentration can be divided into two main classifications - wet and dry. In the former, water is the separating medium, and in the latter (generally confined to coal sizes 3/4-in. or less) air is used as the separating medium. The SO_2 from stacks are removed using scrubbers, mixing coal with calcium carbonate before combustion. Until recently there were no methods developed for complete removal of sulfur in coal or SO_2 from stacks.

The principle problem in coal combustion is the same as it has been for many decades; first, we should know the reaction mechanisms for combustion, and then to interpolate or extrapolate from the well studied coals to predict the behavior of other types of coal. Without this latter ability, we are forced to repeat laborious and time-consuming experiments on all types of coals.

There are a number of problems associated with the study of the thermal decomposition and the oxidation of pulverized coal. Among them are the laboratory simulation of large scale facilities, non-disturbing diagnostic equipment and obtaining meaningful gas samples.

In an effort to overcome these problems, the region behind the reflected shock wave of single pulse shock tube was used in this study. Using this facility, rapid heating of coal particles to elevated temperature, associated with combustion, is possible. The temperatures can be maintained for a short, yet controllable, period of time and subsequently decreased at a rapid rate.

Three coals and three model sulfur compounds were shock heated in nitrogen and dry air. Gas samples were collected after shock heating. During the thermal decomposition of the model organic compounds and the three coals, the yield of H_2S increased with temperature from 900 K to 1450 K and then remained constant to 1550 K. Above 1550 K, the yield of H_2S decreased rapidly with increasing temperature. This decrease in yield above 1550 K is due to the thermal instability of H_2S. Kinetic analysis of data, showed the activation energies of the reactions in organic model compounds were in good agreement with the literature values. Thus the chemical reactions leading to the formation of H_2S were similar in both organic model compounds and coals. From the oxidation of the two organic model compounds, iron pyrites (FeS_2) and three coals, the yield of SO_2 increased with increasing temperature up to 1800 K and was independent of temperature above 1800 K. Kinetic analysis of the data showed the activation energies of the reactions involving model compounds were in close agreement with the literature values. Kinetic analysis of the temperature dependence of the SO_2 yield from iron pyrites and organic model compounds indicated that similar chemical reactions involving sulfur

bonds governed the production of SO_2. Activation energies of the reactions involving coals were in close agreement with the activation energies calculated from surface oxidation rates. Therefore, the overall oxidation of coals govern the emission of SO_2.

2.0 Review of Literature

2.1 Origin

The origin of sulfur in coal has attracted considerable attention with out any definite conclusions having been drawn. There is no definitive evidence of the way sulfur occurs in organic combinations(6), but there is general agreement that organic sulfur compounds are uniformly distributed throughout coal as part of its fundamental constitution. It has been suggested that the most probable and principal source of organic sulfur in coal is the sulfur in the coal-forming plants, but this is unlikely to be the only source. Organic sulfur is stated to be present in molecular combinations as cystin(6) a derivative of plant albumin. It has been also suggested that it occurs partly as thiols, sulphides, and disulphides and partly as ring compounds(7). The fact is that the complex nature of coal has so far resisted critical experiments to establish the nature of the organic sulfur compounds (see Fig. 1).

There has also been much speculation about the origin of iron pyrites in coal. It is probable that pyrites may have been formed in different ways and at different times in the process of coal formation, and that both external and internal sources of sulfur have each played their part. Hydrogen sulfide, evolved through decay of peat bog, would precipitate iron sulfide by reaction with soluble iron compounds, for example, ferrous bicarbonate present in the percolating ground waters. The ferrous sulfide thus precipitated could later be transformed to pryites(8). A second possibility results from the reduction by the

organic matter in the peat or coal bed of ferrous sulfate present

in percolating water or by the contact with iron compounds, not

necessarily soluble, with decaying organic matter. The reduction of

these ferrous compounds would explain the thin coating of pyrites in

coal at shrinkage cracks. It is also possible that iron and sulfur

bacteria have played an important role and are responsible for finely

divided pyrites associated with coal substances.

2.2 Determination of Forms of Sulfur in Coal

Sulfur is generally present in three forms: sulfate, pyritic, and

organic, and the sum of these is reported as the total sulfur. Total

sulfur can be determined by the following three chemical methods,

(1) The Eschka method(21), (2) the bomb-washing method(22), and (3) the

high-temperature combustion method(23).

The Eschka procedure consists of thoroughly mixing coal with a

mixture of magnesium oxide (MgO) and sodium carbonate (Na_2CO_3) and

ashing it in a muffle furnace at 800 C. The sulfur, now in a soluble

form, is leached out with water and precipitated from the resulting

solution as barium sulfate ($BaSO_4$). The precipitate is filtered, ignited

and weighed. This method is rapid when carried out on large batches

of samples. It is most accurate when used for coals containing no more

than 6 or 7% sulfur. This method is discussed in detail in Appendix B.

The bomb washing procedure is convenient for laboratories that make

frequent coal calorimetric determinations as described in ASTM D-2105(21).

In this method a calorimeter bomb is filled with oxygen to a pressure of

20 to 30 atmospheres or at least 5 grams of oxygen per gram of coal.

After the combustion reaction is complete, the calorimeter remains in

the temperature bath for five minutes and then the calorimeter is vented.

The interior of the calorimeter is carefully washed with a solution of

methyl orange, an acid-base indicator. This washing is continued until

there is no further acid reaction, as shown by the color change of the

methyl orange indicator. The washings are collected and the sulfur is

precipitated from the solution as barium sulfate. The precipitate is

filtered, ignited, and weighed.

In the high-temperature combustion method, a weighed amount of coal

is burned in a tube furnace in a stream of oxygen at a temperature of

1350 C. The sulfur oxides are absorbed in a solution of hydrogen

peroxide (H_2O_2) yielding H_2SO_4. The acid solution is titrated with

NaOH, and total sulfur is determined.

Sulfate sulfur is determined by extracting a weighed sample of

coal with dilute HCl followed by precipitation as barium sulfate $(BaSO_4)$.

Sulfate sulfur is soluble in dilute HCl. Pyritic and organic forms of

sulfur are insoluble.

Pyritic sulfur is determined by extracting a weighed sample of

coal with dilute HNO_3 followed by titrimetric determination of iron in

the extract as a measure of pyritic sulfur. Extraction of pyritic sulfur

from coal with dilute HNO_3 involves oxidation of ferrous to ferric

and sulfide sulfur to sulfate, both of which are soluble in HNO_3.

There are drawbacks in this method, such as sulfate sulfur is also soluble in HNO_3 and the amount of pyritic sulfur present in coal is not determined. As a consequence, instrumental methods are being considered to determine the pyritic sulfur in coal.

Some of the instrumental methods are atomic absorption and x-ray diffraction. The HNO_3 extraction of pyrite (FeS_2) from coal yields a solution ideal for the atomic absorption of iron as a measure of pyritic sulfur. In the determination of crystalline pyrite in coal by x-ray diffraction, finely ground coal samples of known pyrite concentration are used as standards in a technique that takes advantage of digital computers for measurement of the diffraction patterns as well as for the calculation of the percentage of pyrite present in the coal sample.

Another method for determining pyritic sulfur is the chemical reduction by lithium aluminum hydride. Pyritic sulfur is reduced to H_2S and then reacted with $CdSO_4$. The H_2SO_4 formed from the reaction is titrated with standard base.

Organic sulfur is determined by the difference:

$$\text{Organic sulfur} = \text{total sulfur} - \left(\begin{array}{c}\text{sulfate sulfur} \\ + \text{ pyritic sulfur}\end{array}\right) \qquad (1)$$

Therefore, any errors made in total, pyritic, or sulfate sulfur determinations will be cumulative in the organic sulfur calculation.

Fig. 1. Occurrence of sulfur in coal.

OCCURRENCE OF SULFUR IN COAL

INORGANIC

ORGANIC

PYRITES

SULPHATES

MERCAPTAN
(RSH)

SULPHIDE
(RSR')

DISULPHIDE
(RSSR')

THIOPHENIC
SYSTEMS
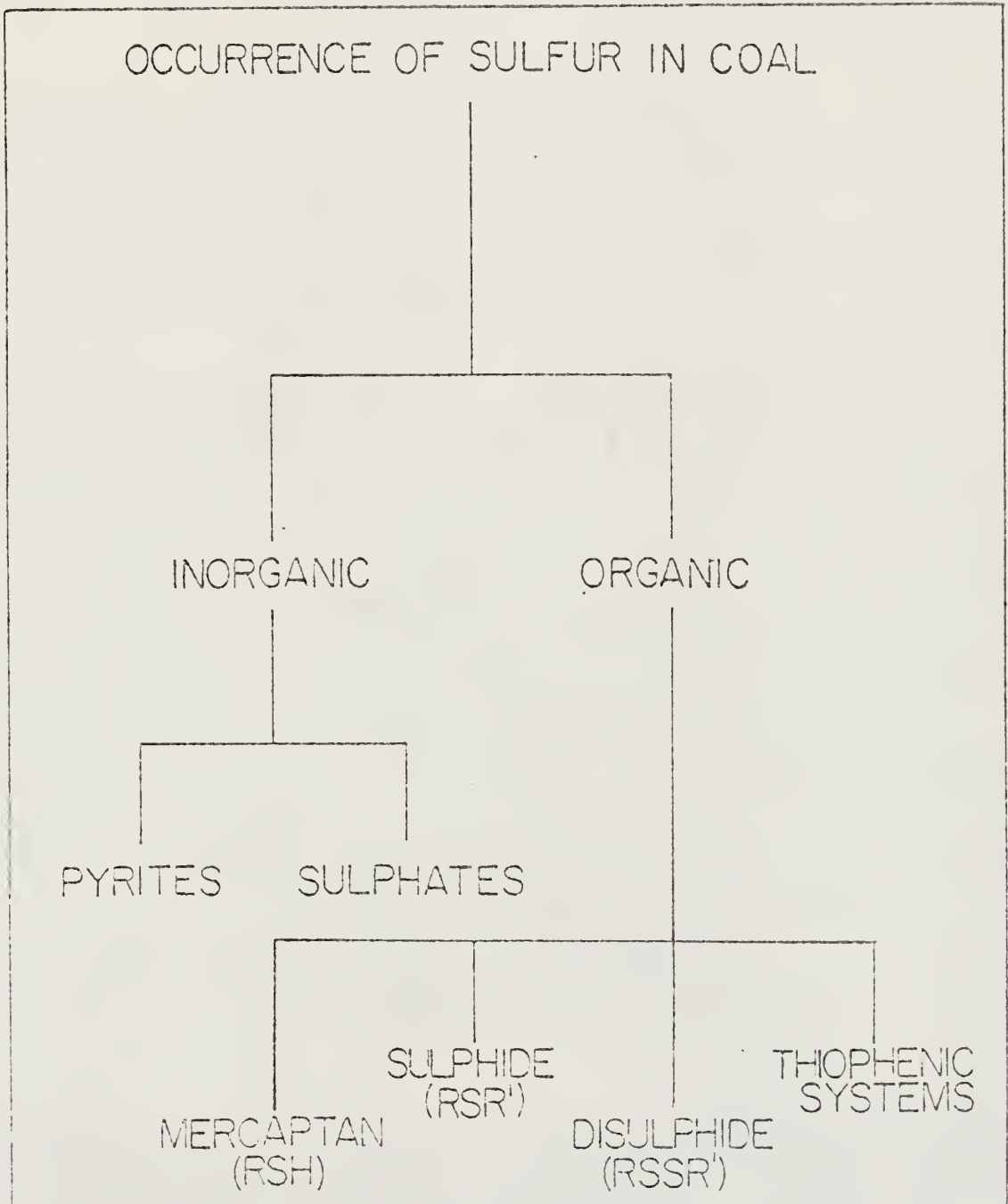
2.3 Iron Sulfide

Inorganic sulfur occurs mainly as disulfide and sulphides. Iron

disulfide (FeS_2) occurs as pryite and marcasite.

Marcasite is a less stable and more reactive form of iron disulfide.

On heating, marcasite transforms to pyrite at 450-500 C. Cubic pyrite

decomposes rapidly at 700 C. Pyrites are attacked rapidly only by

strong oxidizing agents such as concentrated HNO_3 or aquaregia(9).

2.3.1 Decomposition of Iron Pyrites

Schwab and Philins have studied the oxidation, thermal decomposition

and reduction of FeS_2(10). They used pryite with a large specific sur-

face area and carried out the reaction between 400-500 C with oxygen.

By controlling the amount of oxygen they limited the reactions to

$$FeS_2 + 11/4\ O_2 \rightarrow 1/2\ Fe_2O_3 + 2\ SO_2 \tag{2.a}$$

and

$$FeS_2 + 7/2\ O_2 \rightarrow 1/2\ Fe_2(SO_4)_3 + 1/2\ SO_2\ . \tag{2.b}$$
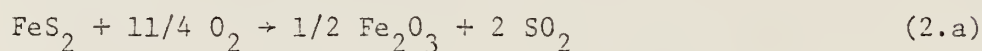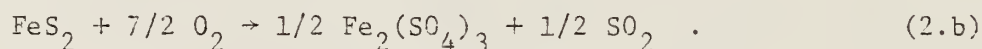
The experiments showed that in the range 400-500 C oxidation of

pyrite proceeds chiefly by reaction (2.a). Sulfate is formed

according to Eq. (2.b). Rates of oxide formation and of total reaction

were found to be nearly independent of temperature. From the kinetic

data, the activation energies for the reactions were found to be 7 to

8 kcal/mole. They inferred that the low values of the activation

energy may be due to the large particle size of the pyrites. As a re-

sult, oxygen diffused slowly through the ferric oxide layer. From the

kinetic data and low activation energies they ascertained that the reaction rate is determined by the rate of diffusion of the oxygen in the ferric oxide layer. The oxidation of pyrite proceeds very rapidly at the air interface.

They found the thermal decomposition of pyrite begins at the homogeneous surface, proceeding at active spots until at about 20% reaction ferrous sulfide separates as a new phase. The phase boundaries thus formed cause an autocatalytic acceleration of the reaction at temperatures below 615 C. An activation energy of 30 kcal/mole was found.

They also found the rate of reduction of pyrite by hydrogen is proportional to the fraction of pyrite remaining to be reduced and has an activation energy of 30 kcal/mole. All surface anions hit by hydrogen molecules and possessing the requisite activation energy react.

In his review article, Attar (18) suggested that pyrite and sulfide are oxidized to a mixture of sulfates and oxides. He suggests that the oxidation occurs by the following sequence of reactions,

$$6FeS_2 + \frac{33}{2}O_2 \rightarrow FeS + FeSO_4 + Fe_2(SO_4)_3 + 7SO_2 + Fe_2O_3) \qquad (3.a)$$

$$5FeS + \frac{21}{2}O_2 \rightarrow FeSO_4 + Fe_2(SO_4)_3 + Fe_2O_3 + SO_2 . \qquad (3.b)$$
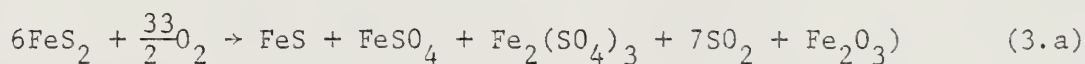
These reactions can occur at temperatures as low as 350-400 C. The reaction mechanism during oxidation of pyrites are dependent upon the temperature, particle size and the kinetic data depend upon the diffusion of oxygen into the ferric oxide layer.

Attar, further concluded, (a) the kinetics of the decomposition were found to depend strongly on gaseous environment and also on the temperature, (b) the decomposition of FeS_2 in any environment is controlled by the availability of $S_2^=$ anions on the surface and from its rate of diffusion from within crystal, (c) in the case of inert carrier gas, the diffusion through the sulfur deficient crystal is smaller than the case where an active carrier gas rapidly reacts with the sulfur on the surface of the crystal.

2.4 Organic Sulfur Compounds

The "organic sulfur" is an umbrella name for a myriad of organic sulfur-containing functional groups. The exact groups which are present in coal are unknown. However, some deductions about their forms may be made. Only divalent organic sulfur is present in coal. This sulfur is present in the form of various organic sulfur groups whose reactivities vary widely (20). The structure of the organic radical which is connected with sulfur atom has a deterministic effect on the rate of the reaction of the sulfur group. The most important divalent sulfur groups in fossil fuels are:

    a) Thiophenes - heteroaromatic compounds
    b) Arylsulfides - sulfur attached to the aromatic ring
    c) Cyclic sulfides - sulfur is a part of a non-aromatic ring
    d) Aliphatic sulfides
    e) Aryl and aliphatic thiols.

2.4.1 Thiophene and its Derivatives

It is a well observed principle that if in any aromatic ring system the vinylidene group, "-CH=CH-" is replaced by a divalent

sulfur atom, -S-, the resulting compound is also aromatic (11).

Thiophene stands in this relation to benzene and is aromatic.

As the consequence of aromaticity, the sulfur atom does not display any of the alkyl or aryl sulfide characteristics(12). The compound undergoes a number of aromatic substitution reactions, in which the nucleus remains stable and the hydrogen atoms are replaced by groups of atoms or other atoms. Thiophene is more reactive towards electrophilic reagents. It readily resinifies or polymerises with oxidizing agents. Thiophenes are very stable and do not thermally decompose up to high temperatures. The products of non-catalytic thermal decomposition are small molecules like sulfur, H_2S, C, and C_2H_4. The gas-phase decomposition follows first order kinetics and has measurable rates at 350-650 C.

The data from some of the laboratories suggest that in high-rank coals thiophenes are the dominant sulfur group. Also during the coalification process, thiols are converted to sulphides, and then to thiophenes. A similar mechanism is believed to occur to part of the organic sulfur during coal pyrolysis(13). Some of the thiols and sulfides are converted into thiophenes. It has been stated that sulphur groups in coal should behave in a similar way to that of the sulfur in model compounds(13).

2.4.2 Sulfides: RSR

These are comparatively stable substances. They do not oxidize in air like mercaptans, but they can be oxidized progressively with

suitable reagents to sulfoxides, sulfones, and sulfonic or sulfinic

acids (11,12).

```
                      O              OH              OH
 R₂S → O      R₂S           R.S.            R.S
                      O            O   O              O
                                   O
 (Sulfoxides)   (Sulfones)   Sulfonic Acid   Sulfinic Acid
     (I)          (II)           (III)           (IV)
```
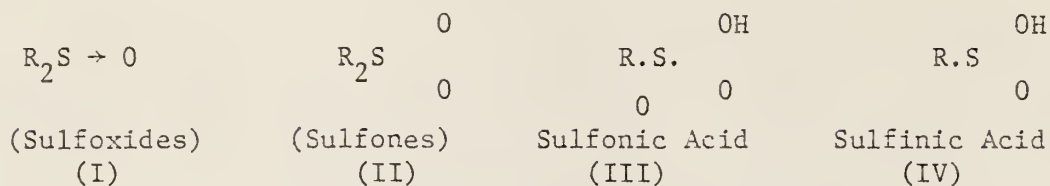
Powerful reagents (e.g., fuming nitric acid, perchloric or chormic

acids) are needed to take reaction beyond stage (I).

The thermal decomposition of sulfides were studied by E. H. Braye

and others (14) in 1955. They investigated the thermal decomposition

of methyl benzyl sulfide in a flow system in the presence of a large

excess of toluene as a carrier gas. From their work, they concluded

that the decomposition of methyl benzyl sulfide is a homogeneous, first-

order reaction with an activation energy of 51($\pm$2) kcal/mole, which they

identified with the dissociation energy of the $C_6H_5 \cdot CH_2 - S \cdot CH_3$ bond. They

carried out these experiments in the temperature range between 742 K to

917 K.

2.4.3 Mercaptans or Thiols (RSH) and Disulfides

These substances are weakly acidic and known for their ease of

oxidation. The lower member of the series are known for their

most unpleasant smell. The arylthiols, such as thiophenol are stronger

acids than phenols. Mercaptans are oxidized slowly in air, the reaction

being catalysed by copper or iron salts (11,12,20).

A. C. Harkness and F. E. Murray (15) studied the gas-phase oxidation

of methyl mercaptan. The reaction between methyl mercaptan and

oxygen in the gas phase has been examined in the temperature range

200-275 C. SO_2 was the main product of the reaction. In the presence

of excess oxygen, complete conversion to SO_2 is obtained at 275 C.

The rate of reaction was found to be strongly accelerated by oxygen and

to be inhibited by mercaptan.

The thermal decomposition of mercaptan was studied by A. H. Sehon

and others (16) in 1954. They studied the thermal decomposition of

benzyl, methyl, and ethyl mercaptans in a flow system, in the presence

of excess of toluene. They concluded from their experiments that the

decomposition is homogeneous, first-order with activation energy of

53($\pm$2) kcal/mole. They identified by the dissociation energy of C-S

bond.

Disulfides are formed readily by the mild oxidation of mercaptans,

and can be reduced back to mercaptans. Their reactions are similar to

mercaptans.

Mercaptans on pyrolysis yield hydrogen sulfide, sulfur, hydro-

carbons, sulfides, and a tarry residue. Diethyl sulfide begins to

decompose at about 400 C. Gaseous hydrocarbons, H_2S and some mer-

captans are formed (17).

Disulfides give a similar range of products and some sulfur. In general it can be said that aliphatic sulfur compounds decompose at an appreciable rate by 500 C.

2.5 Transformation of the Sulfur Compounds in the Gas Phase

The gases considered are:
1) Inert,
2) reducing and,
3) oxidizing gases.

The reactions can occur in the bulk or at the gas solid interface. The gas-solid reactions of FeS_2 were already discussed. In the reactions of the organic groups there are three major differences (18).

1) The gas-phase reaction occurs predominantly in the gases that are fed into the reactor, e.g., H_2. The reaction on the solid occurs in a medium rich in hydrocarbons.
2) The gas-phase reactions have a higher frequency factor than the solid reactions.
3) The residence time of the reactants in the gas is smaller than the organic solid.

Thermodynamics will determine the types and concentrations of sulfur species in the gas above 600 C. Thermodynamics of some of the reactions of the organic sulfur compounds in the gas-phase were examined by Fuchs (19). According to his studies, above 600 K organic sulfur compounds decompose into elemental sulfur, H_2, and carbon. Around 800 K, CS_2, C, and S_2 are formed. In the high temperature pyrolysis H_2S and CS_2 are the main products.

2.6   Coal

In his review article, Attar (18) concludes that the kinetics
and the thermodynamics of H_2S holds the key to the ultimate distribution
of sulfur in coal pyrolysis. He presented the following points of
discussions: 1) most of the sulfur that is volatilized is released
below about 800 C because (a) FeS_2 is reduced almost completely to
FeS and H_2S below 800 C. FeS is rather stable and releases very
little of its sulfur, (b) the rate of reaction of H_2S with the basic
minerals is so large above 700 C that, most of H_2S is trapped,
(c) around 800-860 C hydrodesulfurization becomes impossible, because
of mass transfer limitations. (2) Sulfur that is volatilized above
800 C is released at a rate which is proportional to the rate of
volatilization of the organic material. Most of this sulfur is in
the form of H_2S and CS_2. (3) only a small fraction of the sulfur is
released in the form of organosulfur compounds. At higher temperatures
H_2S and CS_2 are the only stable species that can survive the secondary
reaction in the gas, (4) hydrodesulfurization of coal above 1200-1300 C
results in almost complete gasification of the solid and, naturally,
the almost complete conversion of the sulfur to H_2S. This is because
the dissociation of molecular hydrogen to atoms becomes appreciable.
The rate of attack of H atoms on the organic C-S and C-C bonds is large
and effects an increase in the rate of gasification.

According to Given (20) the stability and other properties of cyclic sulfides mentioned in previous sections show that they should be added to the list of possible types of sulfur compounds in coals. Their behavior on pyrolysis is not reported, but it seems very likely that if they were present in coals, much of the sulfur could be retained in the char on carbonisation, and sulfur would not be released readily from coals during combustion.

Also according to Given (20), on pyrolysis of various sulfur-containing compounds, the sulfur is not always eliminated but becomes built into a large aromatic system. Thus in the case of coal it might be expected that some of the sulfur would remain in the coke.

According to the recent studies by Attar and Dupuis (24) on the distribution of organic sulfur functional groups in coal" they concluded that most of the organic sulfur in coal is present in the form of thiophenic structures. They studied two types of coals, Illinois #6 and Texas lignite and they found 27.4% by weight as aliphatic or alicyclic sulfur, 41.8% by weight as dibenzothiophenic and 30.8% by weight as single thiophenic sulfur in Illinois no. 6 and 26.6% aliphatic or alicyclic, 16.3% dibenzothiophenic and 57.1% as single thiophenic in Texas lignite.

Eric M. Suuberg and other (25) studied the yields, and the composition of products from the pyrolysis of pulverized Montana lignite in a batch reactor. They found that the yields of all volatiles increased monotonically with temperature at a heatup rate of 1000 C/s and

a helium pressure of one atmosphere. The yields of products approached

the following asymptotic values at 1000 C; 16.5% water (including 6.8%

moisture), 9.5% carbon dioxide, 9.4% carbon monoxide, 5.4% tar, 1.3%

methane, 0.6% ethylene, 0.5% hydrogen, and 0.9% ethane, propylene,

propane, benzene, plus traces of other hydrocarbons. Pyrolysis at

1000 C volatilized about 70% of the sulfur and 25% of the nitrogen.

Consequently, the sulfur content (percent by weight) in the char is

lower than that of the lignite.

3.0   Experimental Procedures

The shock tube used in this study was designed and constructed by Seeker (2).   It was modified to a single pulse shock tube in order to collect samples of the gaseous products from the thermal decomposition of coal and model compounds.

3.1   The Shock Tube

The shock tube is a device in which a plane shock wave is produced by the sudden bursting of a diaphragm which separates a gas at high pressure from one at low pressure.   As the result of bursting the diaphragm, a shock front is formed in the low-pressure gas, moves into the test section until it encounters the tube end wall, at which time it is reflected back into itself.   A temperature and pressure increase is associated with the shock wave which is used for thermal processing of the test gas.   Due to the reflection of the shock wave back into itself, an additional increase in temperature and pressure occurs.   The temperature and pressure of the gas behind the reflected shock can be held constant for a few milliseconds.

The movements of the shock front, the contact surface and the rarefraction wave are shown in the distance-time (x-t) diagram in Fig. 2. The diagram illustrates that immediately after the diaphragm is ruptured, the incident shock wave moves into the lower pressure test gas in the test section.   At the same time a rarefraction fan moves in the opposite direction toward the high-pressure region in the driver section.

Figure 2.

A) An x-t diagram showing progress of the incident shock (IS), the
    reflected shock (RS), the rarefaction wave (RW), and the contact
    surface (CS) which separates the driver and test gases. The
    various regions associated with shock wave diagrams are also
    distinguished. The wave diagram is incomplete in that it only
    shows the wave interactions from the diaphragm to the test section
    end wall (2).

B) The temperature distribution at time t_1 (2).
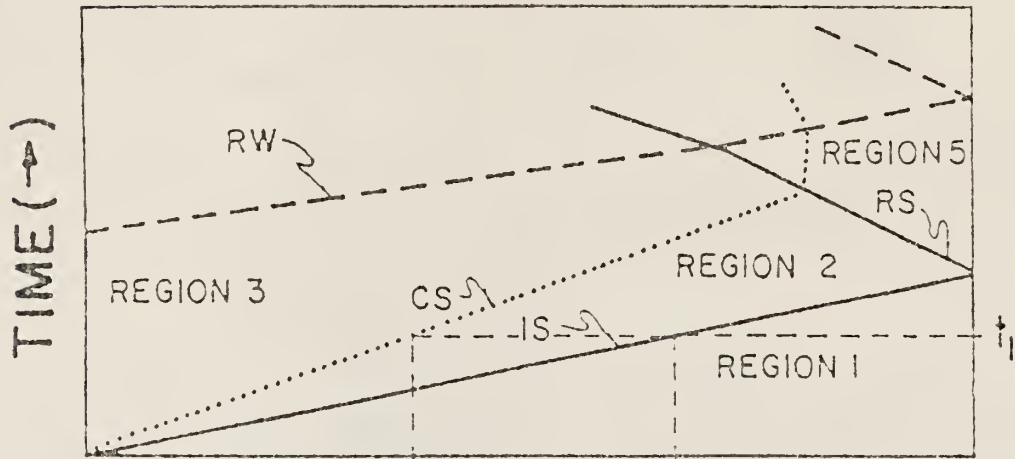
A)
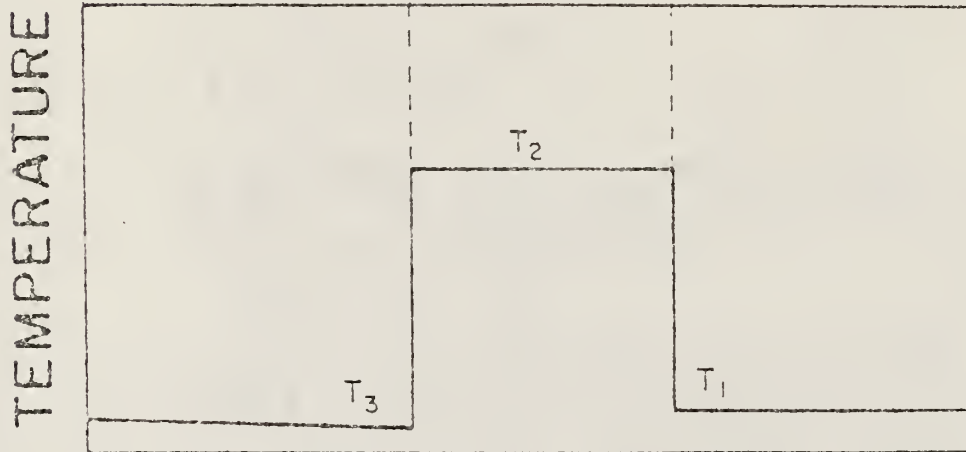
B) DISTANCE

Eventually, the shock front moving in the test-section will hit the end wall and move back towards the diaphragm. The rarefraction head will reflect off the driver end-wall and move into the test-section. The reaction time or "dwell-time" is defined as the time interval at the observation station between passage of the reflected shock and quenching by the rarefaction wave.

The material used for the construction of the tube was 304 stainless steel, with an inner diameter of 5.08 cm and a wall thickness of 0.635 cm. The overall length of the tube is 10 meters. The tube is subsectioned into several different lengths. During this study the tube had a seven meters test section and a 1.86 meter driver section. Throughout this study helium was used in the driver section and zero air and zero nitrogen in the test section.

There are certain diagnostics associated with the facility. The speed of the incident shock is determined with two platinum thin film resistance gauges. The thin film gauges are grouped as close to the test section end-wall as possible, since it is desired to know the speed just before reflection. The gauges are separated by 20.3 cm. This technique can be used to calculate shock speeds and the corresponding shock Mach number to an accuracy of 0.05% (2).

The temperature and pressure behind the reflected shock can be determined by using the following gas dynamic relations and Mach number (5),

$$\frac{T_5}{T_1} = \frac{[2(\gamma-1)M_s^2 + (3-\gamma)][(3\gamma-1)M_s^2 - 2(\gamma-1)]}{(\gamma+1)^2 M_s^2} \quad , \tag{4}$$

and

$$\frac{P_5}{P_1} = \left[\frac{2\gamma M_s^2 - (\gamma-1)}{(\gamma+1)}\right] \left[\frac{(3\gamma-1)M_s^2 - 2(\gamma-1)}{(\gamma-1)M_s^2 + 2}\right] \tag{5}$$

where T_5 is the temperature behind the reflected shock T_1 is the initial temperature of the gas, P_5 is the pressure behind the reflected shock, P_1 is initial pressure of the gas, γ is the specific heat ratio of the test gas, and M_s is the measured Mach number. Equations (4) and (5) are based on the assumptions of a frozen perfect gas (i.e., gas is ideal and there is no dissociation (or ionization) of gas and the gas has no momentum or energy loss).

At this point one has to discuss the real behavior which exists in the experimental work. As it is seen from Fig. 2 that the re-flected shock will reach the contact surface quickly, therefore, the interaction of the shock with this interface, which is the zone of mixing, will cause small secondary waves to move back into the obser-vation region. Due to this, there is a significant change in gas temperature behind the reflected shock. The pressure rise can be seen in Fig. 3. It is basically isentropic and is common to all shock tube experimentation. Due to the isentropic nature of the wave, the change in temperature can be estimated from the pressure

Figure 3. Typical oscillograms showing pressure, laser extinction,
and line emission for (A) oxidation, and (B) pyrolysis of
pulverized coal. (IS - incident shock, RS - reflected shock,
RW - rarefaction wave; calculated reflected shock conditions;
(A) 1500 °K, 6.7 atm, (B) 1400 °K, 7.1 atm: coal - Illinois
#6 (from (2)).

(A) AIR

(B) NITROGEN
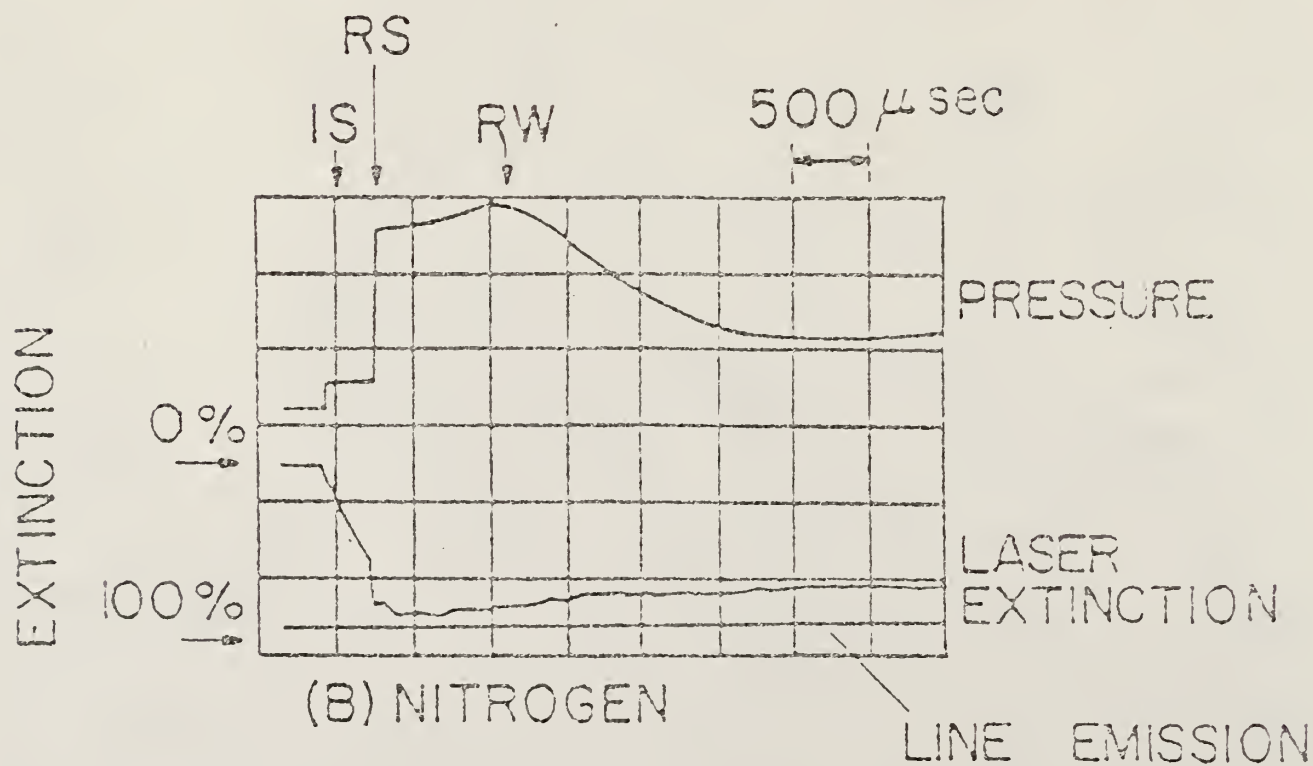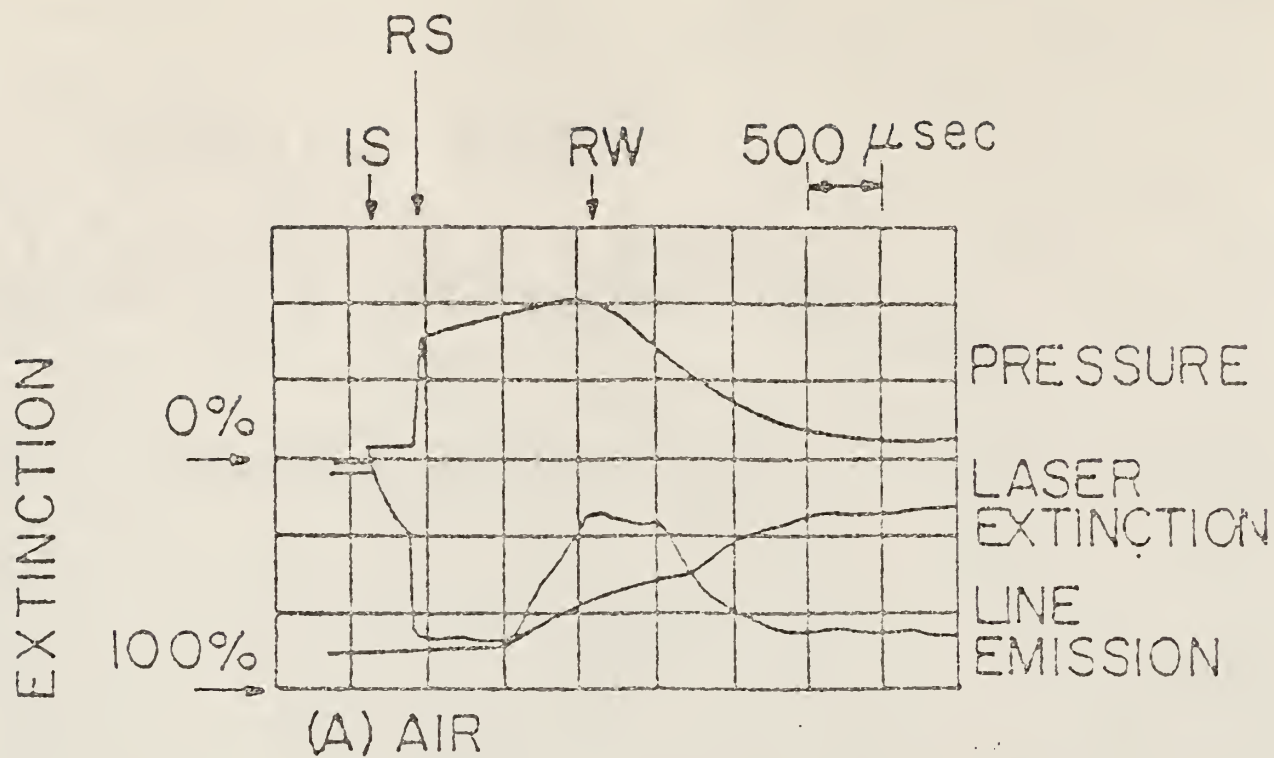
history using the normal isentropic relationship (5)

$$T_5' = T_5 \left(\frac{P_5'}{P_5}\right)^{\frac{\gamma-1}{\gamma}} \tag{6}$$

where the primes indicate the maximum temperature and pressure and
γ the ratio of the test gas specific heats.

In the test section, a four port observation station was installed
about 9 cm from the end-wall. In three of the four ports quartz
windows were installed, and in the fourth port a Kistler piezo-electric
pressure transducer was mounted flush to the inner wall. A beam from
He-Ne laser was passed vertically through two of the quartz windows and
detected by RCA Photomultiplier tube (PMT). The extinction of this beam
was a measure of particle suspension behavior during the experiment.
The emission from the sample was monitored through the third quartz
window. In order to decrease the intensity of the continum emission
from the incandescent coal particles, mylar diffusing screens and
apertures were placed in front of the photo multiplier tube. To
focus the emission on the photocathode of the PM tube, a lens and
aperture configuration is used and is shown in Fig. 4. From the
technque developed by Seeker (2), we can deduce the temperature of
the particle suspension from the emission measurements. Oscillograms
for oxidation and pyrolysis are shown in Fig. 3. This is covered in
detail by Seeker (2).

Figure 4. A cross-sectional view of the diagnostics at the four-
        port observation station where: A-aperture, L-lens,
        IF- interference filter, M - mylar screen (reduces
        intensity), and PMT - photomultiplier tube (from (2)).
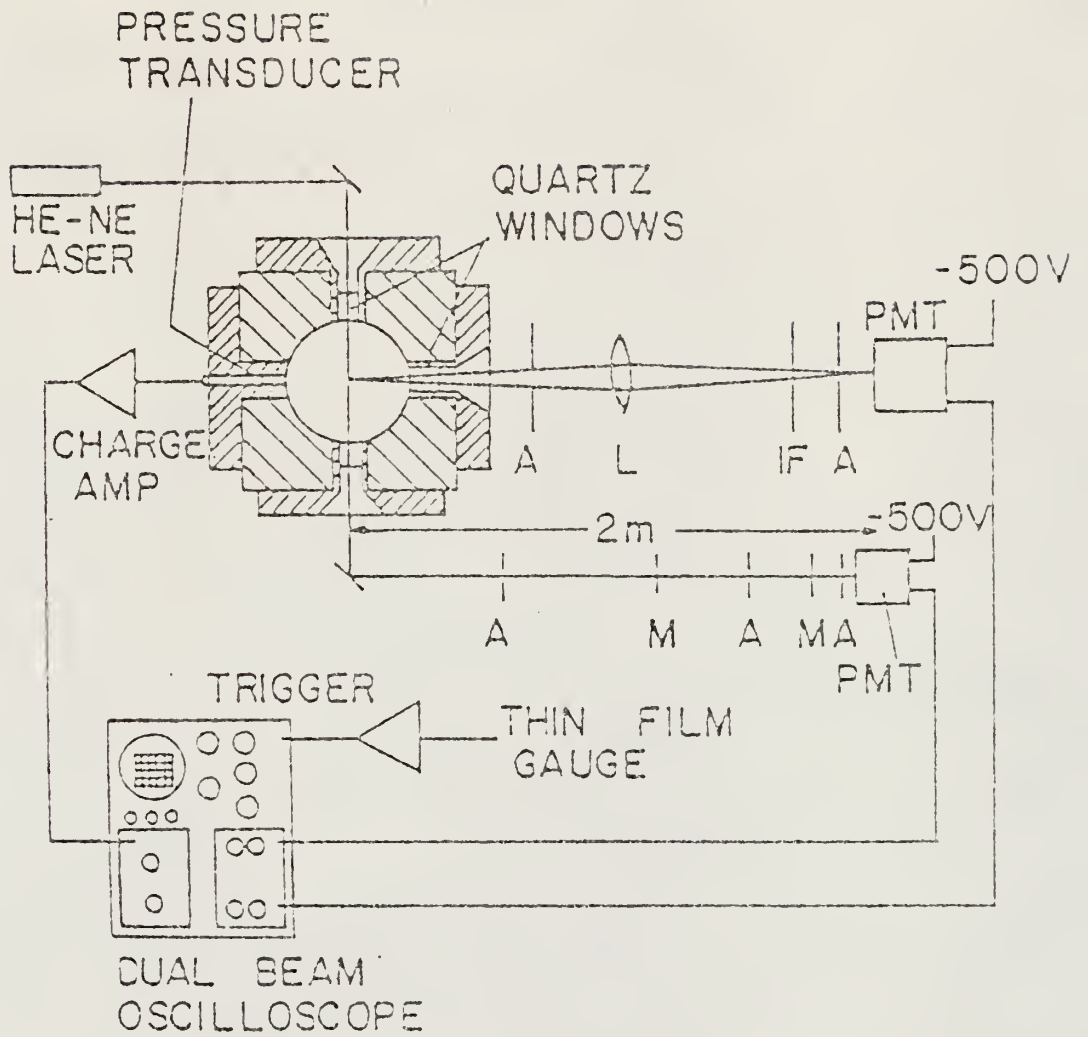
3.2 The Single Pulse Shock Tube

This is similar to the conventional shock tube previously dis-
cussed, with two additional features. A variable length driver and
a dump tank. A schematic of the single pulse shock tube is given in
Fig. 5. Ideally the reaction is allowed to proceed behind the
reflected shock for a known and controllable period of time. This
time period is determined by the arrival of the rarefaction wave
which cools the reaction zone. By changing the length of the driver
section we can control the time of arrival of the reflected rare-
faction at the test section end-wall. In order to prevent the re-
flected shock from again being reflected and re-entering the reaction
zone, a dump tank is used. As soon as the reflected shock arrives at
the intersection of the driver section and the dump tank, the wave
preferentially moves into the dump tank. Because of its low pressure,
the shock is damped out by the sharp area expansion at the dump tank
throat. By making use of the dump tank, a single pulse is attained.

The use of single pulse shock tube allows the reaction to proceed
for only a few milliseconds. Using the isentropic relationship (3),

$$\frac{dT}{dt} = \frac{\gamma-1}{\gamma} \left(\frac{T_5}{P_5}\right) \frac{dP}{dt} \tag{7}$$

the initial rarefaction cooling rate was calculated and was found to be
1.1×10^5 K/sec for N_2 and air test gases and 5×10^5 K/sec for Argon.

The solid samples of 20 mg were inserted into the tube on a
small plate about 1.5 cm in diameter. The plate was suspended from the

Figure 5. Single pulse shock tube diagram (from (2)).
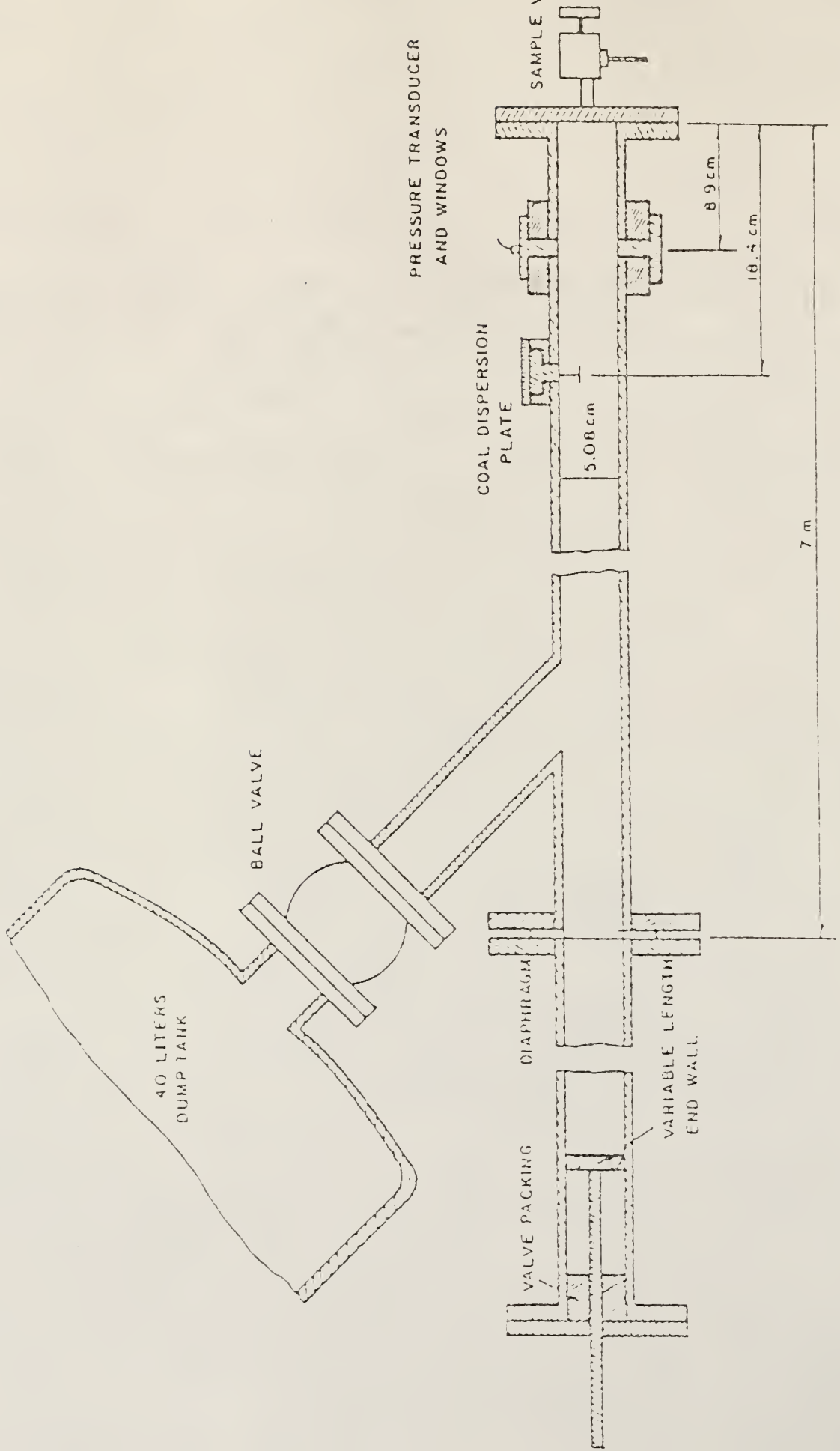
PRESSURE TRANSDUCER
AND WINDOWS

SAMPLE VALVE

COAL DISPERSION
PLATE

8.9 cm

18.4 cm

5.08 cm

BALL VALVE

40 LITERS
DUMP TANK

DIAPHRAGM

VARIABLE LENGTH
END WALL

VALVE PACKING

7 m

end-wall as shown in Fig. 6. The sample dispersion technique was discussed in detail by Seeker (2).

3.3. Coal and Model Compound Samples

The coal samples used in this study along with their proximate analyses are given in Table 1. According to proximate analyses, Illinois No. 6 and Pittsburgh seam have similar volatile matter and Kansas-Missouri has less volatile matter compared to the other two coals. Among the three coals Kansas-Missouri has the highest sulfur content. Coal samples were passed through a standard test sieve of mesh number 400 with a nominal opening of 38.1 μm.

The sulfur containing model compounds used in this study were iron pyrites, L-cystine, and thianthrene. All of these samples were passed through a standard test sieve of mesh number 400 with nominal opening of 38.1 μm. The structure of L-cystine and thianthrene are shown in Fig. 7.

3.4 Wet Chemical Methods

After the test suspension was quenched, gas samples were obtained and analyzed by wet chemical methods. The gas sampling system was designed and constructed by Wegner (4), and is shown in Fig. 8. The gas is passed through the 7 μm filter to prevent any remaining large particles from entering the sampling bottle.

A Varian 90-P gas chromatograph equipped with 6' x 1/8" molecular sieve column was used to determine the extent of driver gas mixing with the test gas. The degree of mixing is determined by the

Figure 6.   Temporal behavior of particulate cloud in the shock
            tube reaction zone.   Cloud dispersion characteristics
            behind the incident shock were determined experimentally
            (from (2)).

POSITION OF COAL INTRODUCTION

CLOUD MAXIMUM DENSITY

OBSERVATION WINDOW

CLOUD TAIL

CLOUD FRONT

TIME (ms)

1·0

0·5

0

REFLECTED SHOCK

INCIDENT SHOCK

20   15   10   5   0

DISTANCE FROM END WALL (cm)

DISPERSION PLATE

QUARTZ WINDOW

.
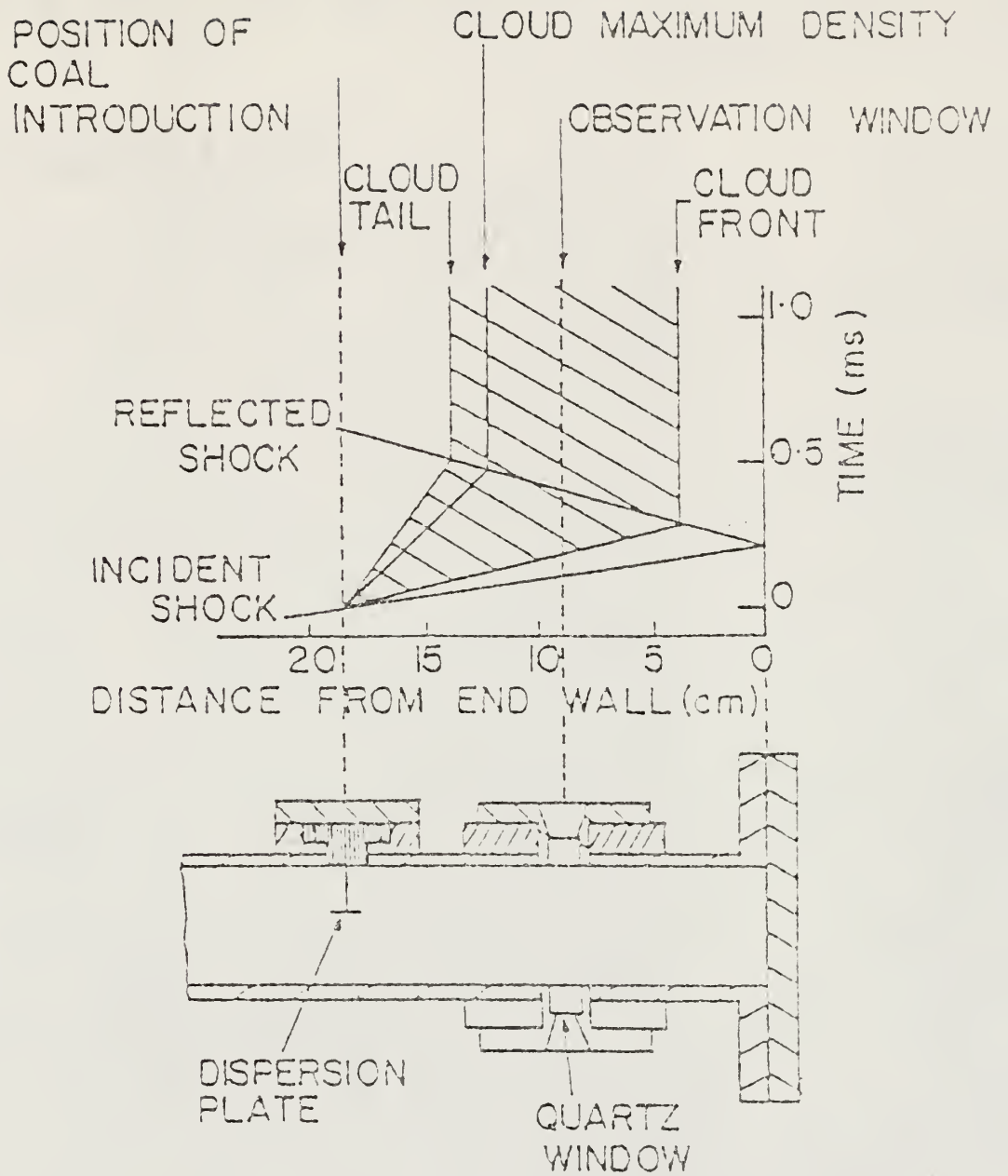
Fig. 7. Structure of the model compounds used in this study.
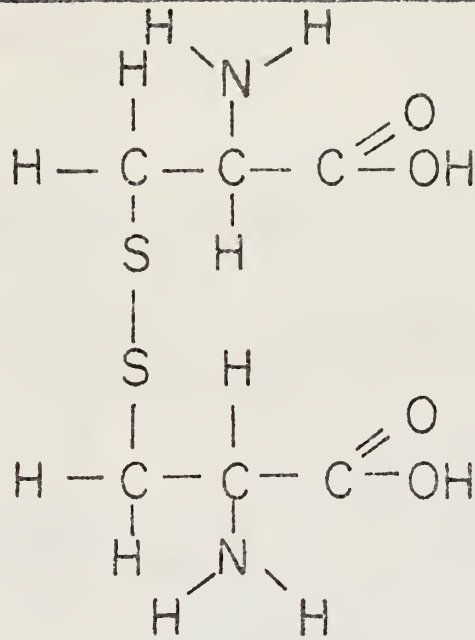
L-CYSTINE
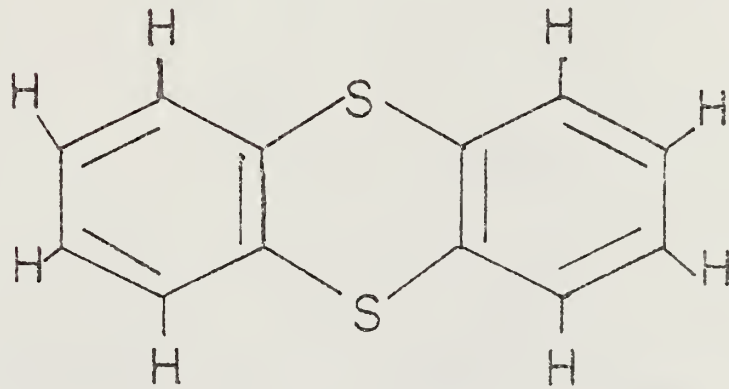
THIANTHRENE

Figure 8. Gas sampling system (from (4)).

TO VENTILATION HOOD

1/4" STAINLESS STEEL TUBING

PRESSURE GAUGE
(KINNEY-MODEL XTG I)

TEST SECTION END WALL

VALVES

SAMPLE BOTTLE
(500cc)

3 WAY VALVE

7-mm FILTER

VACUUM PUMP
(WELCH-MODEL 1400)
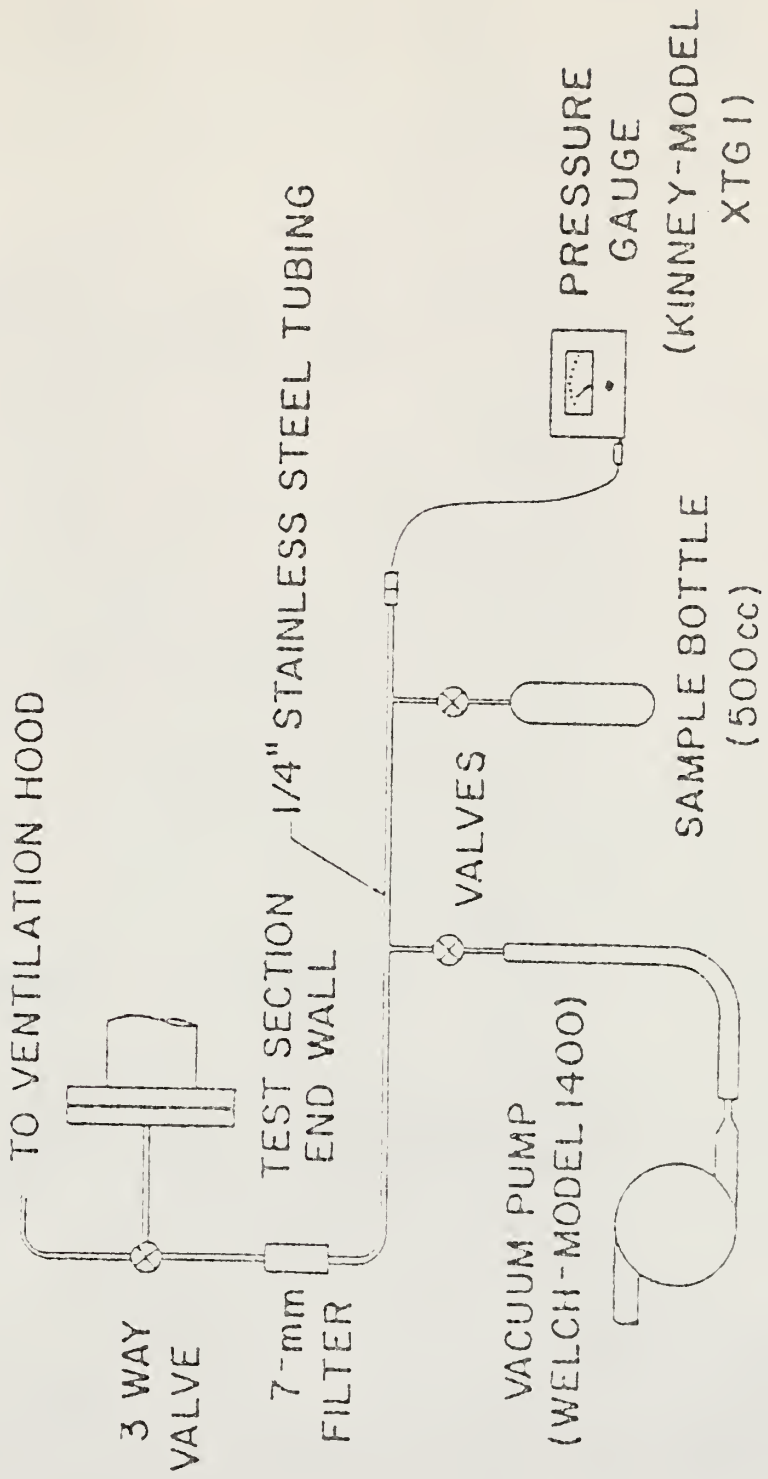
Table 1.   Proximate Analysis as Received (by Hazen Research,
           Inc., Golden, Co.)

	Pittsburgh Seam	Illinois No. 6	Mo-Kansas
Volatile matter	35.5%	34.43%	27.94%
Moisture	1.9%	4.38%	2.34%
Fixed Carbon	56.2%	48.46%	36.84%
Ash	6.4%	12.73%	32.88%

Sample Designation	Total S%	Pyritic S%	Organic S%	Sulfate S%
Pittsburgh Seam	0.96	0.07	0.64	0.25
Illinois #6	3.41	0.42	1.85	1.14
Mo-Kansas	5.27	3.36	1.47	0.44

Sample Dilution Multiplication Factor (SDMF), which is obtained by matching the response of the N_2 peak from a 200 μl injection of the sample gas with the response of the N_2 peak obtained from the injection of pure test gas (N_2 or zero air). Since helium was used for both as a driver gas in the shock tube and also as a carrier gas in the chromatograph, the ratio of the injection volumes yielding equivalent responses was directly relatable to the degree of mixing. The degree of mixing is given by

$$SDMF = \frac{200}{\delta}$$

δ = volume of the test gas injection needed to duplicate a 200 μl sample injection of N_2.

Method of Analysis for SO_2

SO_2 is absorbed by aspirating a measured volume of gas sample through a solution of potassium tetrachloromercurate (TCM). This results in the formation of a dichlorosulfitomercurate complex. To eliminate the interference by heavy metals, "ethylenediaminetetraacetic acid disodium salts (EDTA) is added. After absorption is complete, the complex is allowed to stand for 15 minutes to eliminate interference by ozone. The interference by oxides of nitrogen is prevented by adding sulfamic acid, which destroys the nitrite anion formed from the absorption of oxides of nitrogen. Then the solution is treated with formaldehyde and acid-bleached pararosaniline, containing phosphoric acid to control pH. The bisulfite ion reacts with formaldehyde and pararosaniline to form the intensely colored pararosaniline methyl-

sulfonic acid (28,29). The absorbance is measured on a Cary model-14 spectrophotometer at 548 nm using the expanded scale (0.0-0.1) slide wire. Concentrations up to few ppm can be measured using this method. Details are given in Appendix A.

Method of Analysis for H_2S

A measured volume of gas containing H_2S is aspirated through an alkaline suspension of cadmium hydroxide. The sulfide is precipitated as cadmium sulfide. To minimize the photo-decomposition of precipitated cadmium sulfide Arabinogalatan is added to the cadmium hydroxide slurry prior to sampling. Then a strong acid solution of N, N-dimethyl-p-phenylene diamine and a ferric chloride solution is added. As the result of the reaction between sulfide, the acid of N, N-dimethyl-p-phenylene diamine solution and ferric chloride, a methylene blue is produced. The production of methylene blue is inhibited by reducing agents like SO_2. This interference is eliminated by adding 2-6 drops of ferric chloride and extending the time of reaction to 30-50 minutes. The ozone interference can be eliminated by allowing the cadmium hydroxide suspension to stand for 15 minutes after aspirating the gas sample (28,30). The absorbance is measured on a Cary model-14 spectrophotometer at 670 nm using the expanded scale (0.0-0.1) slide wire. Concentrations of a few ppm or less can be measured using this method. Details are given in Appendix A.

4.0 Results and Discussions

4.1 Pyrolysis

4.1A Model Compounds

The thermal decomposition of the model organic compounds L-cystine
and thianthrene was investigated in the temperature range, 900 K to
1700 K. The yield of hydrogen sulfide increased from 900 K to 1470 K
and then remained constant to 1520 K. Above 1520 K, the yield of H_2S
decreased rapidly with increasing temperature. The yield of H_2S, repre-
sented as a percentage of the weight of the model organic compounds are
plotted as a function of temperature in Fig. 9. The weight percent
of sulfur in L-cystine is 26% and is 29% in thianthrene. At 1520 K,
the fraction of the total sulfur converted to H_2S in L-cystine and
thianthrene is approximately 11% and 2%, respectively. The results
for the pyrolysis of the L-cystine and thianthrene are listed in
Tables 2 and 3.

The kinetic analysis of the data was conducted on the assumption
that the overall decomposition was first-order in sulfur concentration
and exhibits Arrhenius behavior. The rate of production of H_2S is given
by the equation

$$\frac{dx}{dt} = k_{uc} \, y \qquad\qquad (8)$$

Fig. 9. H_2S yields as a percent weight of the model organic
compounds, verses the maximum particle temperature
for L-cystine and Thianthrene.
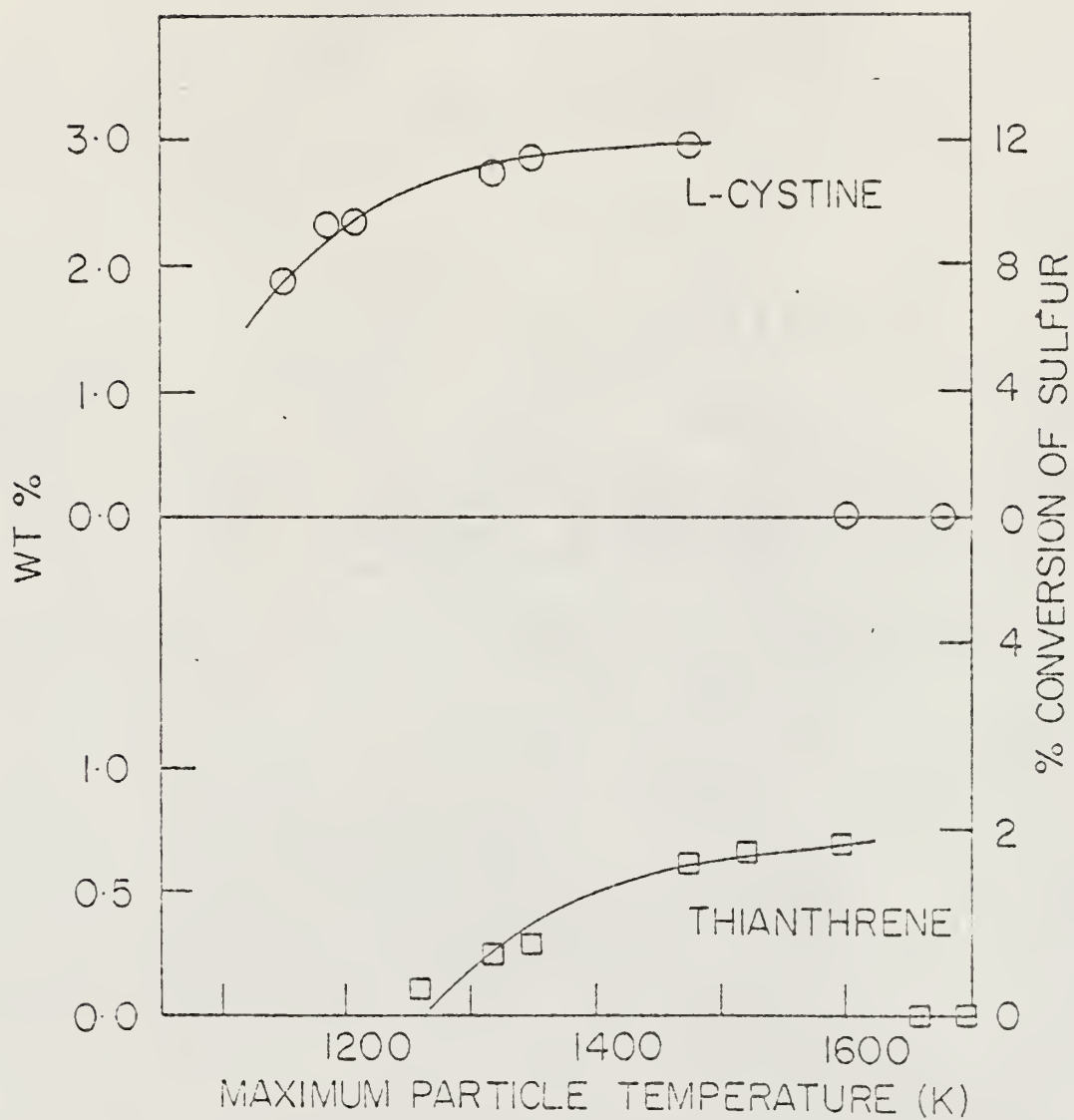
Table 2.   L-cystine $[-SCH_2CH\,(NH_2)\,COOH]_2$ Pyrolysis.

Maximum Particle Temperature T(K)	$\frac{1}{T}\times 10^4$ (K^{-1})	Δt μs	PPM of H_2S x Present	y (PPM)	Wt%	$\ln[\frac{1}{y}\frac{x}{\Delta t}]$
1150	8.60	1500	80	100	1.87	6.27
1185	8.40	1500	130.25	49.75	2.303	7.46
1210	8.26	1300	161.4	18.6	2.305	8.80
1320	7.50	1250	169.2	10.8	2.72	9.46
1350	7.40	1300	175.0	5.00	2.84	10.42
1475	6.77	1400	180.00	0.0	2.97	-
1600	6.25	1350	0.0	0.0	0.0	-
1680	5.95	1500	0.0	0.0	0.0	-

Table 3. Thiantherene (C_6H_4S C_6H_4S) Pyrolysis.

Maximum Particle Temperature T(K)	$\frac{1}{T} \times 10^4$ (K^{-1})	Δt μs	PPM of H_2S x Present	y (PPM)	Wt%	$\ln[\frac{1}{y} \frac{x}{\Delta t}]$
1300	7.69	1200	10.0	53.58	0.1298	5.04
1320	7.50	1300	14.09	49.49	0.2269	5.38
1350	7.40	1200	17.5	46.08	0.2672	5.75
1475	6.70	1500	42.66	20.92	0.609	7.21
1520	6.50	1350	55.00	8.54	0.6429	8.46
1600	6.25	1400	63.58	0.0	0.6602	-
1660	6.02	1450	0.0	0.0	0.0	-
1700	5.88					

where x is the concentration of H_2S in ppm, y is the difference in the maximum yield of H_2S and the yield at a particular temperature, k_{uc} is the uncorrected reaction rate constant and t is time. Throughout the experimental work the pressures were maintained at 7 ± 1 atm and the reaction times were maintained at 1400 ± 200 μsec. Expressing the above equation in logarithmic form,

$$\ln \left(\frac{dx}{dt} \frac{1}{y} \right) = \ln k_{uc} \ . \tag{9}$$

Since we assumed that the reaction exhibits Arrhenius behavior, we can substitute the Arrhenius expression for the rate constant k_{uc},

$$\ln k_{uc} = \ln A - E_{exp}/RT \tag{10}$$

where A is a constant, k_{uc} is the uncorrected reaction rate constant, T is the temperature of the gas in degrees K, R is gas constant, and E_{exp} is the activation energy. Substituting (10) into (9), we have

$$\ln \left(\frac{dx}{dt} \frac{1}{y} \right) = \ln A - E_{exp}/RT \ . \tag{11}$$

A plot of $\ln \left(\frac{dx}{dt} \frac{1}{y} \right)$ vs $\frac{1}{T}$ gives a straight line with slope $(-E_{exp}/R)$ from which we can calculate the uncorrected activation energies.

For the accurate kinetic data interpretation, one has to account for the contribution from additional reactions occurring in the cooling-off period. Thus, the reaction contribution in the cooling period was calculated and the correction for the rate constants were made using the method proposed by Tschuikow-Roux (32).

The rate of disappearance of the reactant, N, during the cooling period is given by

$$\frac{-dN\,(t)}{dt} = N(t)\ A\ \exp\ [-E/RT(t)]\ . \tag{12}$$

N is the number of moles of reactants at any time t. The decrease in pressure, which is proportional to time is given by

$$P(t) = P_5 + (dP/dt)\ (t-t_1) \tag{13}$$

where

t_1 is the time at which the cooling time begins,

P_5 is the total pressure of the compressed and heated gas at temperature T_5, and

$\frac{dP}{dt}$ is a constant.

Since the pressure wave is isentropic, the initial rarefaction cooling rate, as calculated from the experimentally observed rate of pressure decrease, is given by the isentropic relationship, Eq. (7)

$$m = \frac{dT}{dt} = \left(\frac{\gamma-1}{\gamma}\right)\frac{T_5}{P_5}\left(\frac{dP}{dt}\right)\ . \tag{7}$$

m was found to be 1.1×10^5 K/sec for nitrogen and air test gases.

Now we define

$$\Delta T = T_5 - T(t)\ , \tag{14}$$

and hence

$$\frac{1}{T(t)} = 1/[T_5(1-\Delta T/T_5)]\ ,$$

$$\approx (1+\Delta T/T_5)/T_5\ . \tag{15}$$

In view of Eqs. (13)-(15),

$$\frac{\Delta T}{T_5} = 1 - [1 + \left(\frac{\gamma}{\gamma-1}\right) \frac{m}{T_5} (t-t_1)]^{(\gamma-1)/\gamma}$$

$$= - \frac{m}{T_5} (t-t_1) + \frac{1}{(\gamma-1)} \frac{m^2}{T_5^2} \frac{(t-t_1)^2}{2i!}$$

$$\approx - \frac{m}{T_5} (t-t_1) \tag{16}$$

Introducing Eqs. (15) and (16) into (12) and integrating we obtain the relative loss of reactant during the cooling process.

$$\ln(\frac{N_1}{N_2}) = A \int_{t_1}^{t_2} \exp \{- \frac{E}{RT_5} [1- \frac{m}{T_5} (t-t_1)]\} \, dt$$

$$= -A \frac{R}{E} \frac{T_5^2}{m} e^{-E/RT_5} [1-e^{-E\Delta T'/RT_5^2}]$$

$$= -k_c \, \varepsilon \tag{17}$$

where $k_c = A\exp (-E/RT_5)$ is the true rate constant at temperature T_5 and

$$- \varepsilon = \frac{RT_5^2}{Em} [1-\exp (- \frac{E}{R} \frac{\Delta T'}{T_5^2})] \tag{18}$$

where

N_1 is the number of moles of reactant at the start of the cooling process, i.e., at t_1

N_2 is the number of moles at t_2 when the reaction rate has decreased to some specified value.

If this value is taken as 10^{-2} of the reaction rate at T_5, then

$$\Delta T' = T_5 - T(t_2)$$

$$= 2T_5^2/[2T_5 + E/(R\ln 10)] \tag{19}$$

In Eq. (17) the quantity N_1 is unknown. Since only N_2 can be determined from product analysis, then we can relate N_1 to N_0, the initial number of moles at $t=t_0$, before any chemical reaction takes place. Now by adding the term $\ln(N_2/N_0)$ to both sides of Eq. (17); thus

$$\ln (N_1/N_0) = \ln (N_2/N_0) - k_c \; \epsilon.$$

Since we assumed first-order reaction

$$\ln (N_1/N_0) = -k_c \; t,$$

and

$$\ln (N_2/N_0) = -k_{uc} \; t_1$$

where k_{uc} is the uncorrected rate constant.
and

$$k_c = (1 + \epsilon/t_1)^{-1} k_{uc} \tag{20}$$

Using Eq. (20) we can calculate the corrected rate constant and thus determine the true activation energy by plotting $\ln k_c$ vs $\frac{1}{T}$. This is shown in Fig. (10) for organic model compounds during pyrolysis.

The values of the activation energy are 52 kcal/mole for L-cystine and 55 kcal/mole for Thianthrene, which are in good agreement with values at lower temperature. According to E. H. Braye and others (14) the thermal decomposition of sulfides in the temperature range of 742 K to 917 K, has an activation energy of 51 ($\pm$2) kcal/mole. From the studies of A. H. Sehon and others (16), the thermal decomposition of mercaptan in

Fig. 10. Plots of ln k_c verses $\frac{1}{T}$ K^{-1} for organic model
compounds during pyrolysis
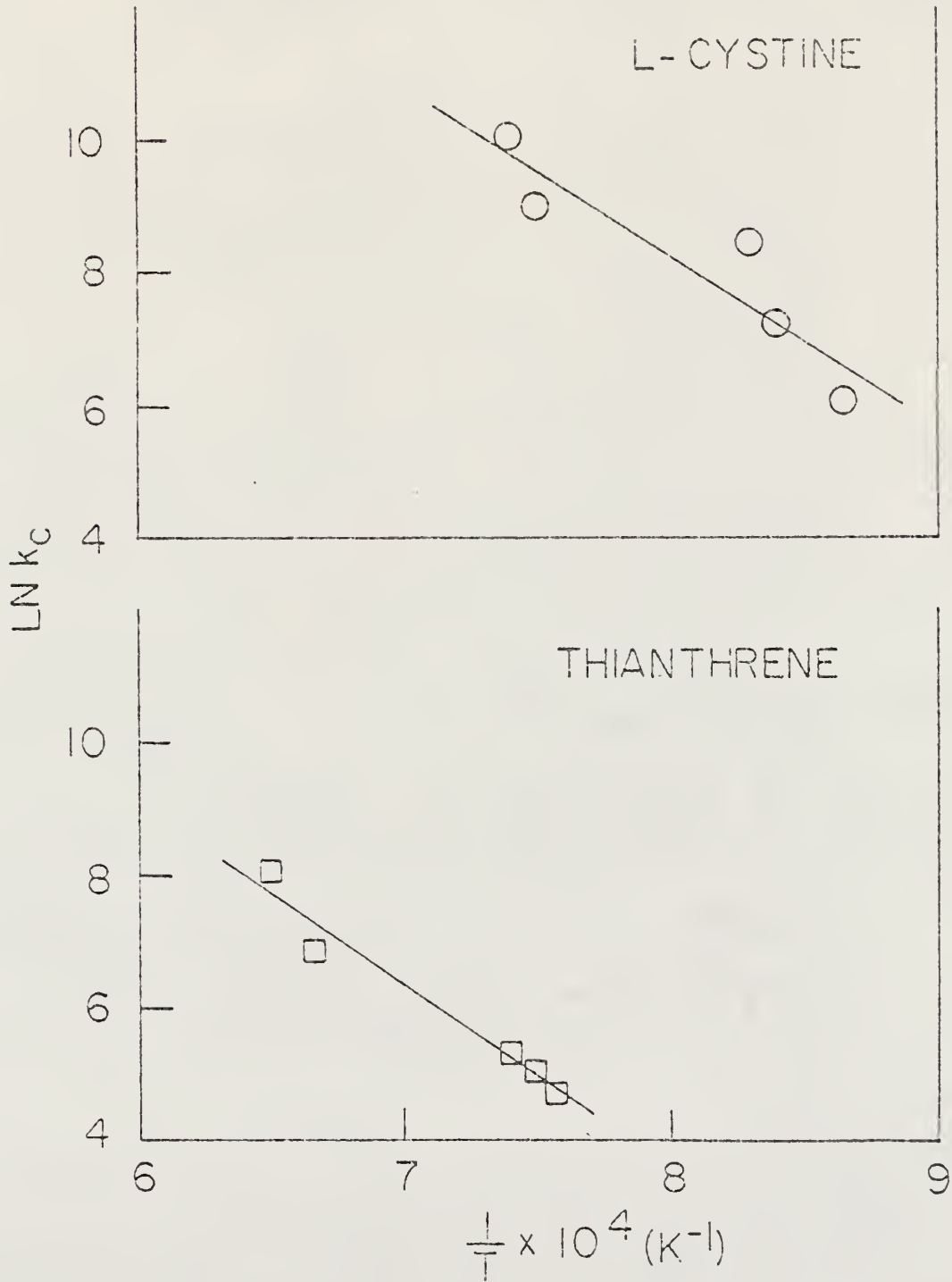
the temperature range of 760 K to 900 K had an activation energy of 53 ($\pm$2) kcal/mole.

4.1B Coals

The thermal decomposition of the three types of coals was investigated in the temperature range, 900 K to 1700 K. The yields of hydrogen sulfide increased from 900 K to 1470 K and then remained constant to 1520 K. Above 1520 K, the yield of H_2S decreased rapidly with increasing temperature. The yields of H_2S represented as a percentage of the weight of the coal sample are plotted as the function of temperature in Fig. 11. Similar to the model compounds, the amount of sulfur converted to H_2S at 1520 K is significantly less than the original amount present in the coals. The amount of sulfur in Pittsburgh Seam, Illinois #6, and the KS-MO coals are approximately 2%, 4%, and 6%, respectively (Table 1). The extent of conversion was 50%, 37%, and 33% for the Pittsburgh Seam, Illinois #6, and KS-MO, respectively. The results for the pyrolysis of the three coals are listed in Tables 4, 5, and 6.

Kinetic analysis of the data was performed in a similar manner as was done in the case of model compounds. From the plot $\ln k_c$ vs $\frac{1}{T}$ which is shown in Fig. 12, we can estimate the true activation energies for these coals.

From these plots we determined an activation energy of 50 kcal/mole for Pittsburgh Seam, 54 kcal/mole for Illinois #6, and 50 kcal/mole for KS-MO. The activation energies obtained for the test coals were similar

Fig. 11.   H$_2$S yields, as a percent weight of the original coal
           sample, verses the maximum particle temperature for
           Pittsburgh seam, Illinois #6, and Mo-Kan.
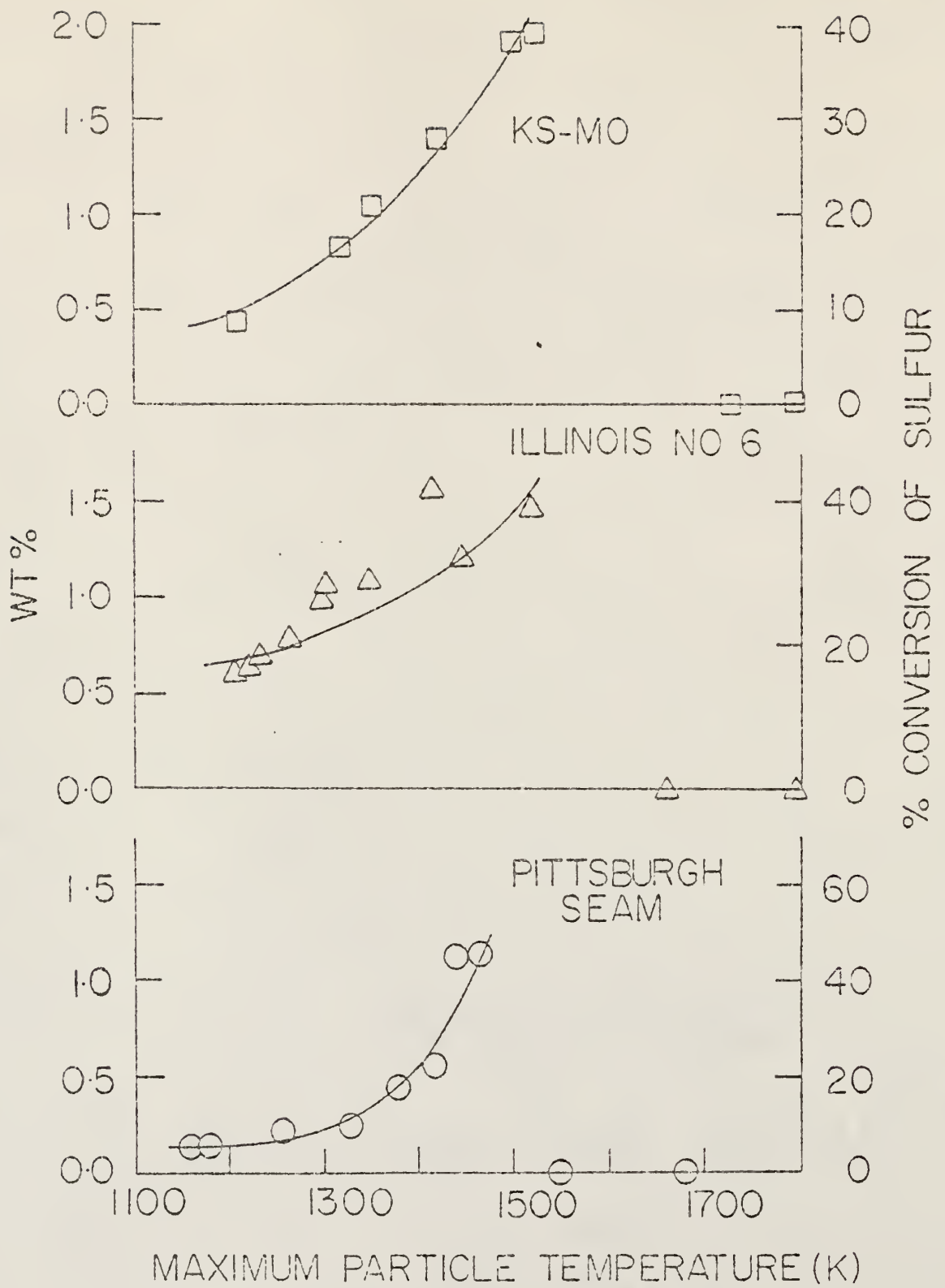
Table 4. Illinois No. 6 Pyrolysis.

Maximum Particle Temperature T (K)	$\frac{1}{T} \times 10^4$ (K^{-1})	Δt μs	PPM of H_2S x Present	y (PPM)	Wt%	$\ln\left[\frac{1}{y}\frac{x}{\Delta t}\right]$
1210	8.26	1600	27.36	97.94	0.6006	5.16
1220	8.19	1400	38.42	86.88	0.6187	5.75
1240	8.06	1400	39.60	85.70	0.668	5.80
1265	7.90	1500	69.60	55.70	0.813	6.72
1300	7.60	1400	86.40	38.90	1.00	7.36
1305	7.66	1400	79.68	45.62	1.08	7.12
1350	7.40	1400	96.07	29.23	1.098	7.76
1445	6.90	1500	116.38	8.92	1.209	9.07
1520	6.57	1500	125.30	0.0	1.464	–
1660	6.02	1600	0.0	0.0	0.0	–
1800	5.55	1625	0.0	0.0	0.0	–

Table 5. Pittsburgh Seam Pyrolysis.

Maximum Particle Temperature T(K)	$\frac{1}{T} \times 10^4$ (K^{-1})	Δt μs	PPM of H$_2$S x Present	y (PPM)	Wt%	$\ln[\frac{1}{y}\frac{x}{\Delta t}]$
1160	8.62	1400	11.0	97.0	0.1428	4.39
1180	8.47	1400	11.5	96.5	0.1493	4.44
1260	7.93	1450	15.0	93.0	0.2045	4.71
1330	7.50	1400	15.0	93.0	0.2415	4.74
1380	7.20	1450	45.0	63.0	0.4383	6.195
1420	7.04	1400	57.0	51.0	0.5552	6.68
1440	6.94	1400	107.0	1.0	1.12	11.24
1465	6.82	1500	108.0	0.0	1.122	–
1550	6.45	1500	0.0	0.0	0.0	–
1680	5.95	1600	0.0	0.0	0.0	–

Table 6. KS-MO Pyrolysis.

Maximum Particle Temperature T (K)	$\frac{1}{T} \times 10^4$ (K^{-1})	Δt μs	PPM of H_2S x Present	y (PPM)	Wt%	$\ln[\frac{1}{y}\frac{x}{\Delta t}]$
1210	8.26	1450	30.625	75.695	0.4375	5.63
1320	7.57	1450	52.66	53.66	0.8207	6.531
1350	7.40	1400	70.10	36.22	1.06	7.231
1420	7.04	1450	79.28	27.04	1.41	7.611
1500	6.60	1400	103.45	2.87	1.91	10.15
1520	6.57	1500	106.32	0.0	1.98	–
1675	5.97	1500	0.0	0.0	0.0	–
1800	5.55	1600	0.0	0.0	0.0	–

Fig. 12. Plots of ln k_c verses $\frac{1}{T}$ K^{-1} for three coals during
pyrolysis.
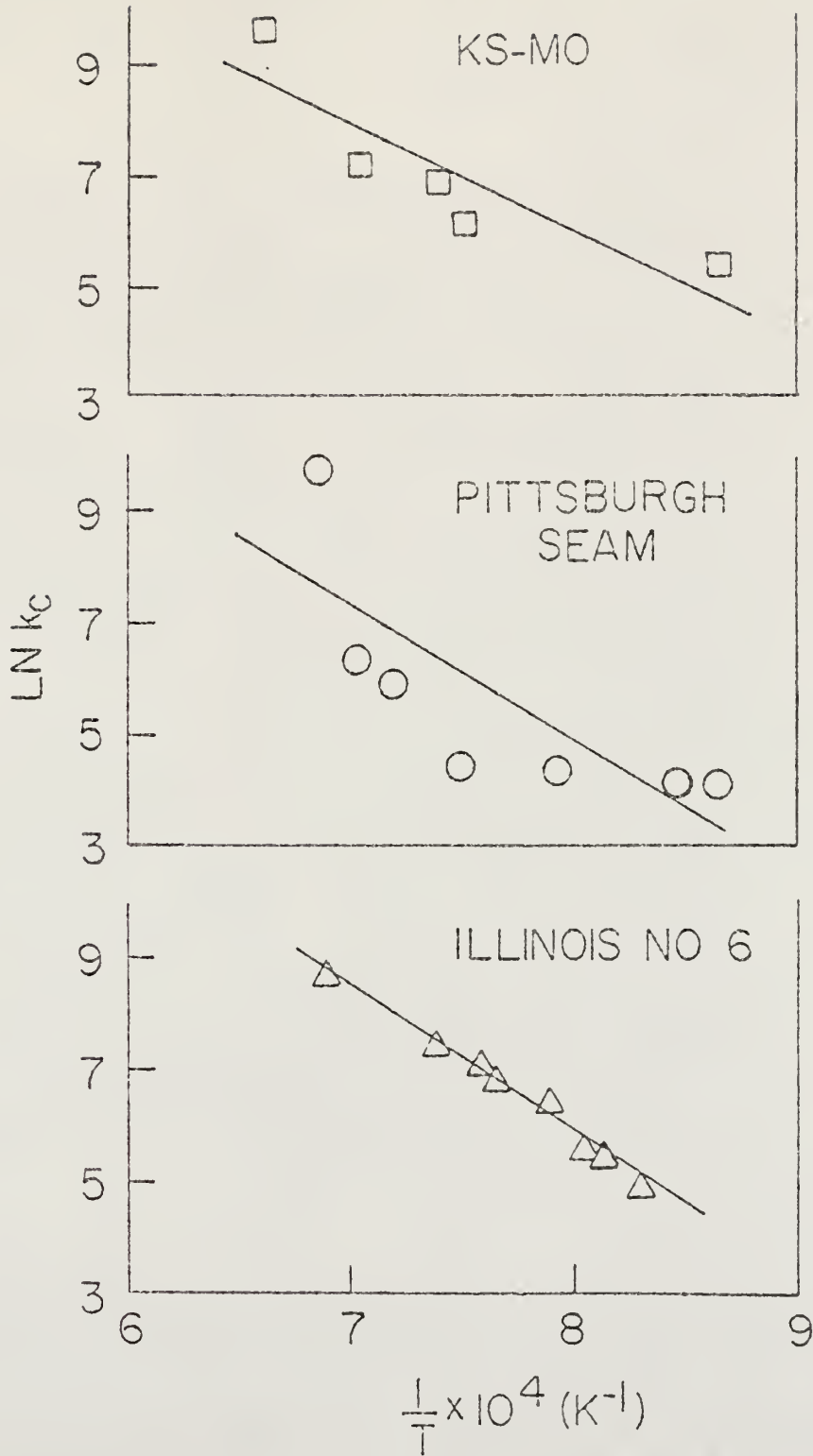
to the activation energies obtained for organic model compounds. This
suggests that the chemical reactions leading to formation of H_2S were
the same in all cases.

4.2   Oxidation

   4.2A   Model Compounds

The two organic model compounds and iron-pyrites (FeS_2) were oxidized
in air over the temperature range, 1175 K to 2200 K. The yields of SO_2
increased with increasing temperature up to 2100 K and was independent
of temperature above 2100 K. The yields of SO_2, represented as a per-
centage of the weight of the initial model compound, are plotted as the
function of temperature in Fig. 13. As can be seen from Fig. 13,
essentially all of the sulfur present in the model compounds is converted
into SO_2 at 2100 K. The results from the oxidation of the model compounds
were shown in Tables 7, 8, and 9.

The kinetic analysis of the data was conducted on the assumption
that the reaction involved are all first-order in model compounds and
obey Arrhenius behavior. According to first-order kinetics

$$\frac{dx}{dt} = k_{uc} [y][O_2] \qquad (21)$$

where x is the amount of SO_2 concentration in ppm, y is the difference
in the maximum yield of SO_2 and the yield at a particular temperature, k_{uc}
is the uncorrected reaction rate constant, and O_2 is the concentration of
oxygen, which is essentially constant because the concentration of
oxygen in the reaction zone does not change significantly during the course
of the reaction.

Fig. 13. SO$_2$ yields, as a percent weight of the original
model compound sample, verses average burning
temperature for L-cystine, Thianthrene, and Iron-
pyrites.
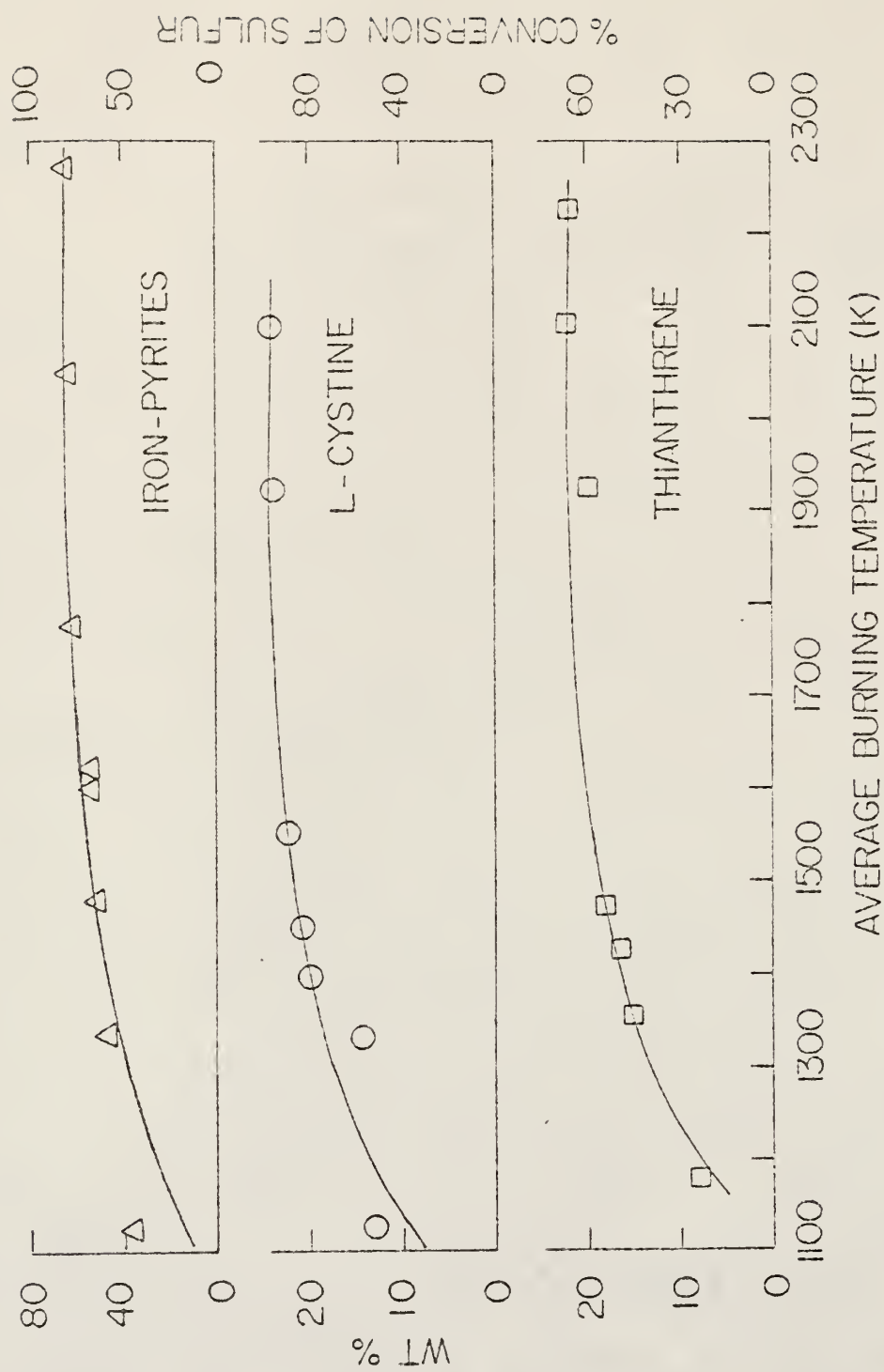
Table 7. L-cystine $[-SCH_2CH(NH_2)COOH]_2$ Oxidation.

Average Burning Temperature T (K)	$\frac{1}{T} \times 10^4$ (K^{-1})	Δt μs	PPM of SO_2 x Present	y (PPM)	Wt%	$\ln[\frac{1}{y}\frac{x}{\Delta t}]$
1125	8.88	1300	900.35	1479.65	13.21	6.148
1335	7.49	1100	1200.00	1180.00	14.69	7.042
1400	7.14	1250	1520.00	860.00	19.65	7.24
1450	6.89	1400	1835.00	545.00	20.95	7.78
1550	6.45	1400	2100.74	279.26	22.52	8.58
1925	5.19	1400	2318.35	62.00	23.80	10.19
2100	4.76	1450	2380.00	0.0	24.12	

Table 8. Thiantherene [C_6H_4S C_6H_4S] Oxidation

Average Burning Temperature T (K)	$\frac{1}{T}\times10^4$ (K^{-1})	Δt μs	PPM of SO_2 x Present	y (PPM)	Wt%	$\ln[\frac{1}{y}\frac{x}{\Delta t}]$
1160	8.62	1200	355.10	2636.20	3.652	4.72
1175	8.51	1300	375.69	2615.43	8.00	4.704
1355	7.38	1400	970.772	2020.34	15.214	5.838
1425	7.01	1400	1098.01	1893.11	16.67	6.026
1480	6.75	1500	1209.4	1781.72	18.33	6.114
1925	5.19	1400	1858.30	1132.81	19.95	7.062
2100	4.76	1500	2530.00	461.12	21.02	8.204
2225	4.49	1400	2940.15	50.97	21.59	10.626
2226	4.496	1400	2991.12	0.0	21.97	

Table 9. Iron Pyrites (FeS$_2$) Oxidation.

Average Burning Temperature T (K)	$\frac{1}{T} \times 10^4$ (K^{-1})	Δt μs	PPM of SO$_2$ x^2 Present	y (PPM)	Wt%	$\ln[\frac{1}{y}\frac{x}{\Delta t}]$
1125	8.88	1300	2230.16	7469.5	36.59	5.442
1335	7.49	1400	3212.25	6446.91	48.77	5.874
1480	6.75	1500	3419.30	6240.36	51.82	5.9006
1600	6.25	1350	4350.00	5309.66	53.26	6.408
1625	6.15	1450	4886.45	4773.21	53.25	6.559
1780	5.61	1400	6200.00	3459.66	60.63	7.154
1950	5.12	1200	6450.00	3209.66	63.18	7.423
2050	4.87	1350	6500.00	3159.66	63.66	7.325
2275	4.40	1200	8779.42	800.24	64.49	9.025
2350	4.25	1300	9659.66	0.0	65.00	

Therefore, Eq. (12) can be written as

$$\frac{dx}{dt} \frac{1}{y} = k'_{uc}, \tag{22}$$

where k'_{uc} is the product of the uncorrected rate constant and the concentration of oxygen. Expressing the above equation in logarithmic form, we have

$$\ln \left[\frac{dx}{dt} \frac{1}{y}\right] = \ln k'_{uc} . \tag{23}$$

Since we assumed that the reaction exhibits Arrhenius behavior and we have defined k'_{uc} as the product of the uncorrected rate constant and the oxygen concentration, we can make the following substitution for k'_{uc},

$$\ln k'_{uc} = \ln A' - E_{exp}/RT \tag{24}$$

where A' is a constant, E_{exp} is the activation energy, T the temperature of the gas, and R is universal gas constant. Substituting Eq. (24) into Eq. (23), we have

$$\ln \left[\frac{dx}{dt} \frac{1}{y}\right] = \ln A' - E_{exp}/RT . \tag{25}$$

A plot of $\ln \left[\frac{dx}{dt} \frac{1}{y}\right]$ vs $\frac{1}{T}$ gives a straight line with slope $(- E_{exp}/R)$ from which we can calculate the uncorrected activation energies. And making the correction for the cooling period and calculating the corrected rate constant k_c as discussed earlier and plotting $\ln k_c$ vs. $\frac{1}{T}$ from which the true activation energy is calculated. This is shown in Fig. 14.

From these calculations we determined an activation energy of 10 kcal/mole for iron-pyrites, 19 kcal/mole for L-cystine and 20 kcal/

Fig. 14. Plots of ln k_c vs $\frac{1}{T}$ K^{-1} for the model
compounds during oxidation.
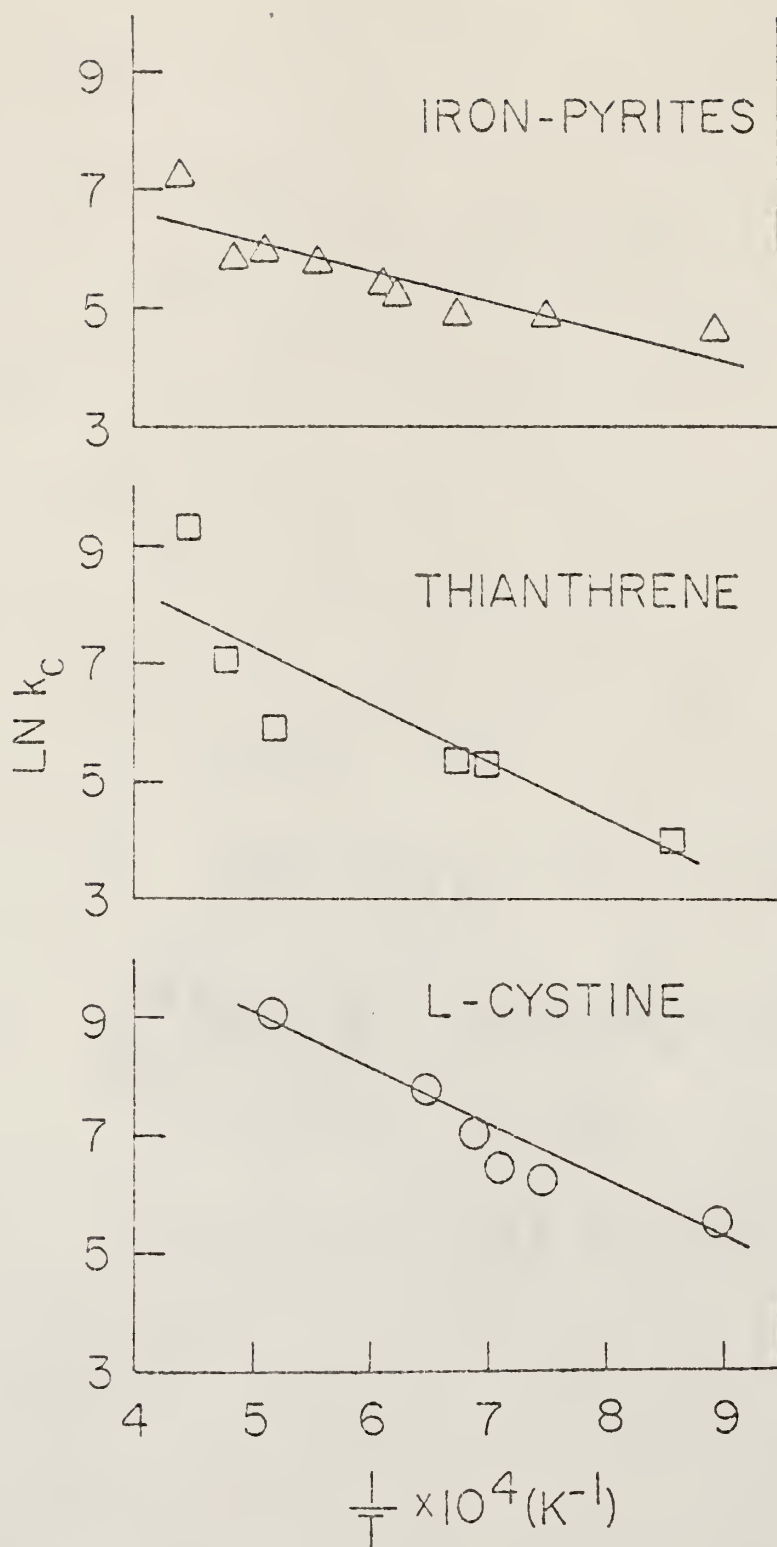
mole for Thianthrene. The value of activation energy obtained for iron-pyrite is compared with the value of 7 to 8 kcal/mole by Schwab and Philins (10) in the temperature range of 400 to 500 C. They suggested the low value of activation energies was due to the particle size of the iron-pyrites and diffusion of oxygen into ferric oxide layer. However, in our experiments, we decreased the diffusion problem by making use of 38.1 μ particles of FeS_2. The values reported by Bateman and Hargrave (26) in their oxidation studies of cyclohexyl methyl sulfide by various peroxides and in various solvents at 50 C found activation energies varying from 6 to 17 kcal/mole. Dankleff et al. (27) in their studies on the oxidation of thioxane by peroxides in various solvents reported activation energies varying from 13 to 20 kcal/mole. The activation energies are in reasonable agreement with the literature values. Thus, the temperature dependence of the SO_2 yields from the organic model compounds and iron-pyrites indicated that similar chemical reactions involving the sulfur bond, governed the production of SO_2.

The true effect of oxygen partial pressure on the reaction was determined via a series of oxidation runs using test gases with different oxygen concentrations in nitrogen. The oxygen concentration was varied from 10% to 30% while maintaining the total gas pressure at 7 ± 1 atm and the gas temperature at 1950 ± 100 K for thianthrene. The measured rate of production of SO_2 is plotted as a function of the oxygen concentration in Fig. 15. The rate for the production of SO_2 was assumed to be of the form

Figure 15. Effect of oxygen partial pressure on the rate of production of SO_2 from the organic model compound (Thianthrene).
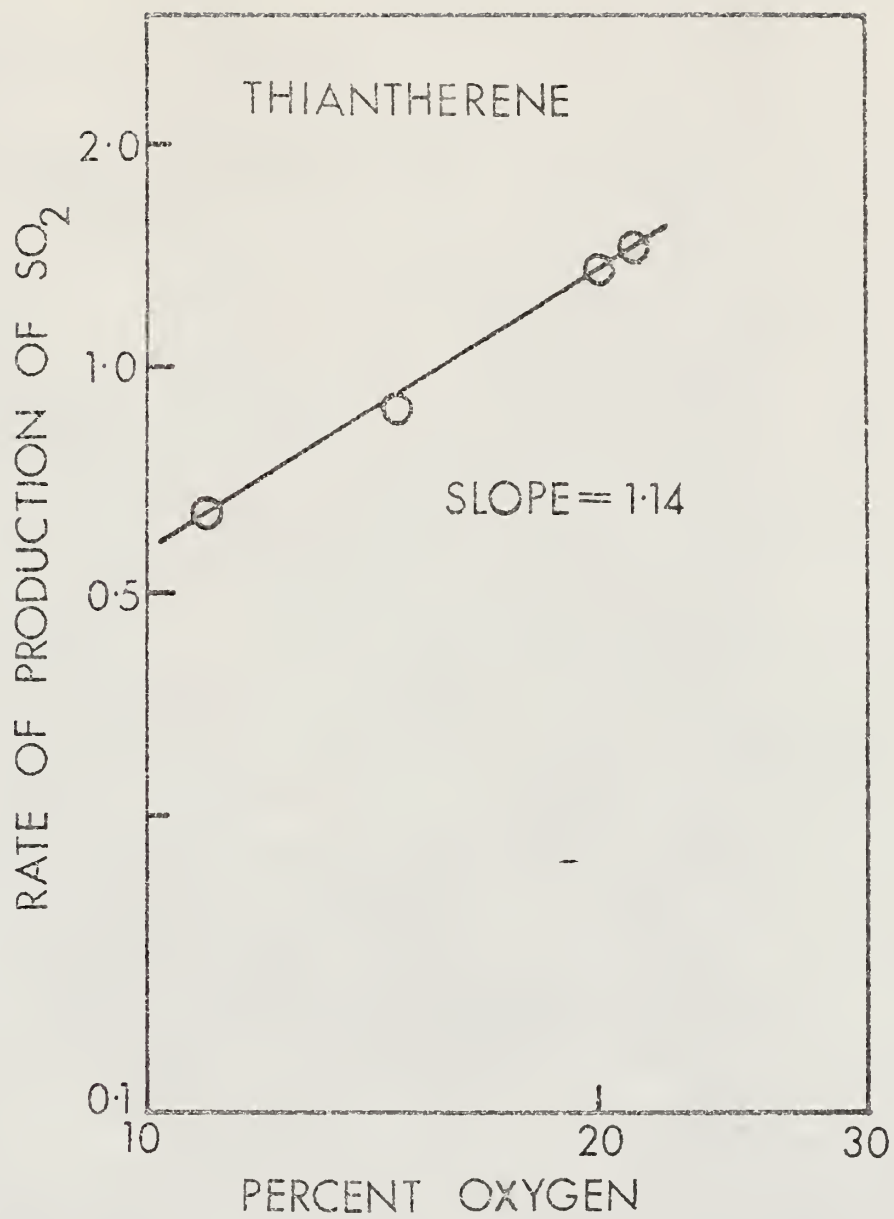
$$R = yC_{O2}^n \ A \ exp \ (-E/RT) \qquad (26)$$

where C_{O2} is the oxygen concentration in the free stream and n is
the order with respect to oxygen. Taking the logarithm of both sides
yields

$$log \ R = n \ log \ C_{O2} + logy \ A \ exp \ (-E/RT) \qquad (27)$$

Therefore, a log-log plot of R versus C_{O2} at a constant temperature
should have the order as the slope. The slope of the data in Fig. 15
was determined to be 1.14. However, it was observed that the maximum
particle temperature increased with increasing oxygen concentration so
that the true order is expected to be less than 1.14, but not significantly
lower than first order.

4.2B Coals

Three coals were oxidized in air over the temperature range, 1175 K
to 2150 K. The yield of SO_2 increased with increasing temperature up to
2100 K and was independent of temperature above 2100 K. The results of
SO_2 yields represented as a percentage of the weight of the initial coal
are plotted as a function of temperature in Fig. 16. As we can see from
Fig. 16, all of the sulfur present in coal is converted into SO_2 at
temperatures above 2100 K. The results from the oxidation of three coals
were shown in Tables 10, 11, and 12. Throughout this experimental work
the pressure of 7 ± atm and reaction times of 1400 ± 200 were maintained.

The kinetic analysis of the data was performed in a similar method as
in the case of model compounds oxidation assuming first-order in the

Fig. 16. SO_2 yields as a percent weight of the original
coal sample, verses average burning temperature
for Pittsburgh Seam, Illinois #6, and Mo-Kan.
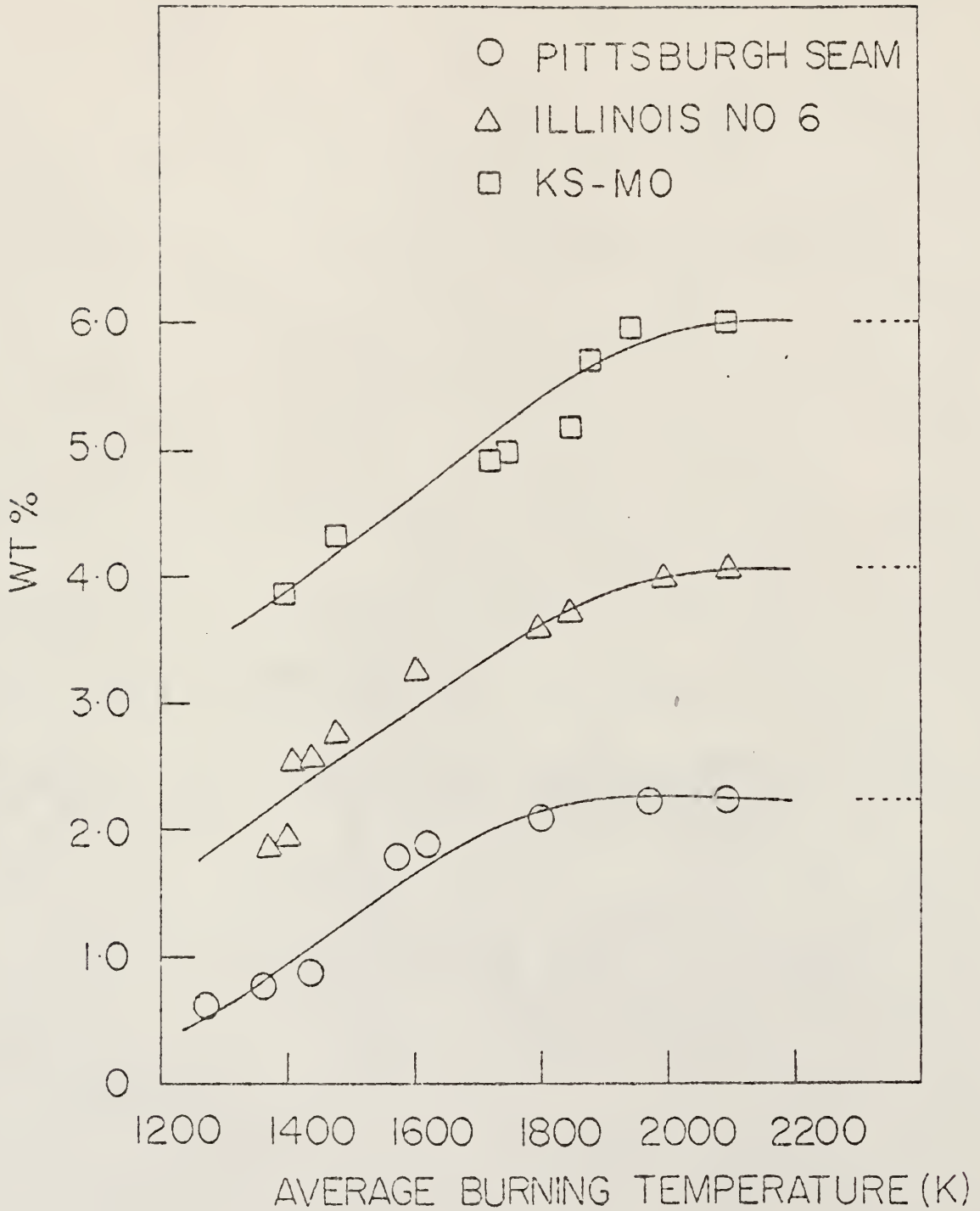
Table 10. Illinois No. 6 Oxidation

Average Burning Temperature T (K)	$\frac{1}{T} \times 10^4$ (K^{-1})	Δt μs	PPM of SO$_2$ x Present	y (PPM)	Wt%	$\ln\left[\frac{1}{y}\frac{x}{\Delta t}\right]$
1375	7.27	1200	125.03	354.27	1.8755	5.16
1400	7.14	1300	138.44	340.86	1.946	5.601
1410	7.09	1300	157.86	321.44	2.55	5.934
1440	6.94	1400	190.86	288.44	2.57	6.188
1475	6.77	1300	248.16	231.14	2.79	6.716
1610	6.21	1300	360.96	118.34	3.28	7.76
1800	5.55	1200	420.98	58.32	3.65	8.7
1860	5.376	1400	457.63	21.67	3.75	9.63
2000	5.00	1200	470.82	8.46	4.01	10.74
2100	4.76	1400	479.30	0.0	4.10	

78

Table 11. Pittsburgh Seam Oxidation.

Average Burning Temperature T (K)	$\frac{1}{T} \times 10^4$ (K^{-1})	Δt μs	PPM of SO_2 x Present	y (PPM)	Wt%	$\ln[\frac{1}{y}\frac{x}{\Delta t}]$
1275	7.84	1300	31.5	280.00	0.519	4.46
1365	7.32	1475	101.25	210.25	0.751	5.80
1440	6.94	1300	161.95	149.95	0.762	6.723
1575	6.34	1400	250.45	61.05	1.836	7.982
1625	6.15	1400	261.85	49.65	1.92	8.234
1800	5.55	1425	281.25	30.25	2.06	8.783
1825	5.47	1350	296.25	15.3	2.17	9.57
1975	5.06	1200	305.20	6.3	2.21	10.60
2100	4.76	1300	311.50	0.0	2.28	

Table 12. Ks-Mo Oxidation

Average Burning Temperature T (K)	$\frac{1}{T} \times 10^4$ (K^{-1})	Δt μs	PPM of SO$_2$ x Present	y (PPM)	Wt%	$\ln\left[\frac{1}{y}\frac{x}{\Delta t}\right]$
1400	7.14	1325	180.9	433.75	3.79	5.75
1480	6.75	1350	349.9	264.75	4.27	6.88
1725	5.79	1300	415.51	199.50	4.82	7.37
1750	5.70	1400	518.71	95.94	4.91	8.25
1850	5.40	1375	579.64	35.01	5.38	9.396
1880	5.31	1400	588.67	25.98	5.70	9.69
1950	5.12	1400	602.33	12.32	5.91	10.45
2100	4.76	1500	614.65	0	6.01	0

remaining sulfur in the coal and Arrhenius behavior. From the plot of ln k_c vs $\frac{1}{T}$ which is shown in Fig. 17, we can calculate the true activation energies involved in three coal types.

From these plots we obtained an activation energies of 38 kcal/mole for Pittsburgh Seam, 40 kcal/mole for Illinois No. 6, and 39 kcal/mole for KS-MO. The activation energies were in agreement with the activation energies calculated from surface oxidation rates by Seeker (2). The true effect of oxygen partial pressure on the reaction was determined via a series of oxidation runs using gases with different oxygen concentrations in nitrogen. The oxygen concentration was varied from 10%-30% while maintaining the total gas pressure at 7 ± 1 atm and the gas temperature at 1950 ± 100 K for the Illinois No. 6 coal sample. The measured rate of production of SO_2 is shown as a function of oxygen concentration in the log-log plot of Fig. 18. The reaction rate was assumed to be of the form given by Eq. (26). Therefore, a log-log plot of R verses C_{O2} at a constant temperature should have the order as the slope. The slope of the data in Fig. 18 was determined to be 0.406. However, it was observed that the maximum particle temperature increased with increasing oxygen concentration so that the true order is expected to be less than 0.406. Specifically, the maximum particle temperature reached in the 10.10% oxygen mixture was between 2700 to 2900 °K but for the 49.0% oxygen mixture runs the temperature was between 3200 to 3350 °K (2). Therefore, the corresponding average burning temperatures were about 2400 °K and 2250 °K, respectively. Therefore, the rates obtained with 49.05% oxygen were higher than the 10.10% points by a factor of

Fig. 17. Plots of ln k_c verses $\frac{1}{T}$ K^{-1} for the
three coals during oxidation.
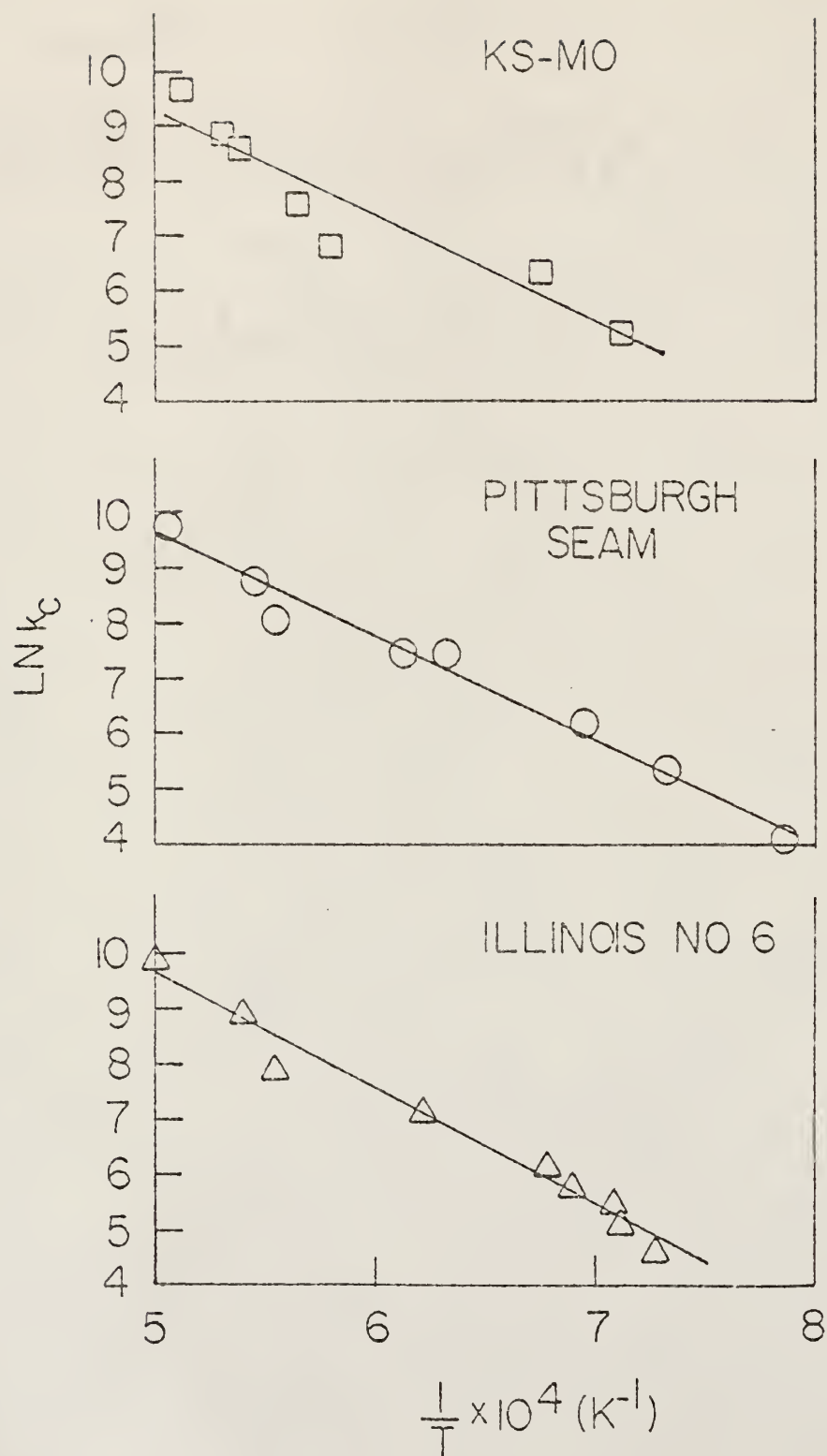
Figure 18 . Effect of Oxygen Partial Pressure on the rate
of production of SO_2 from a coal sample (Illinois
#6).
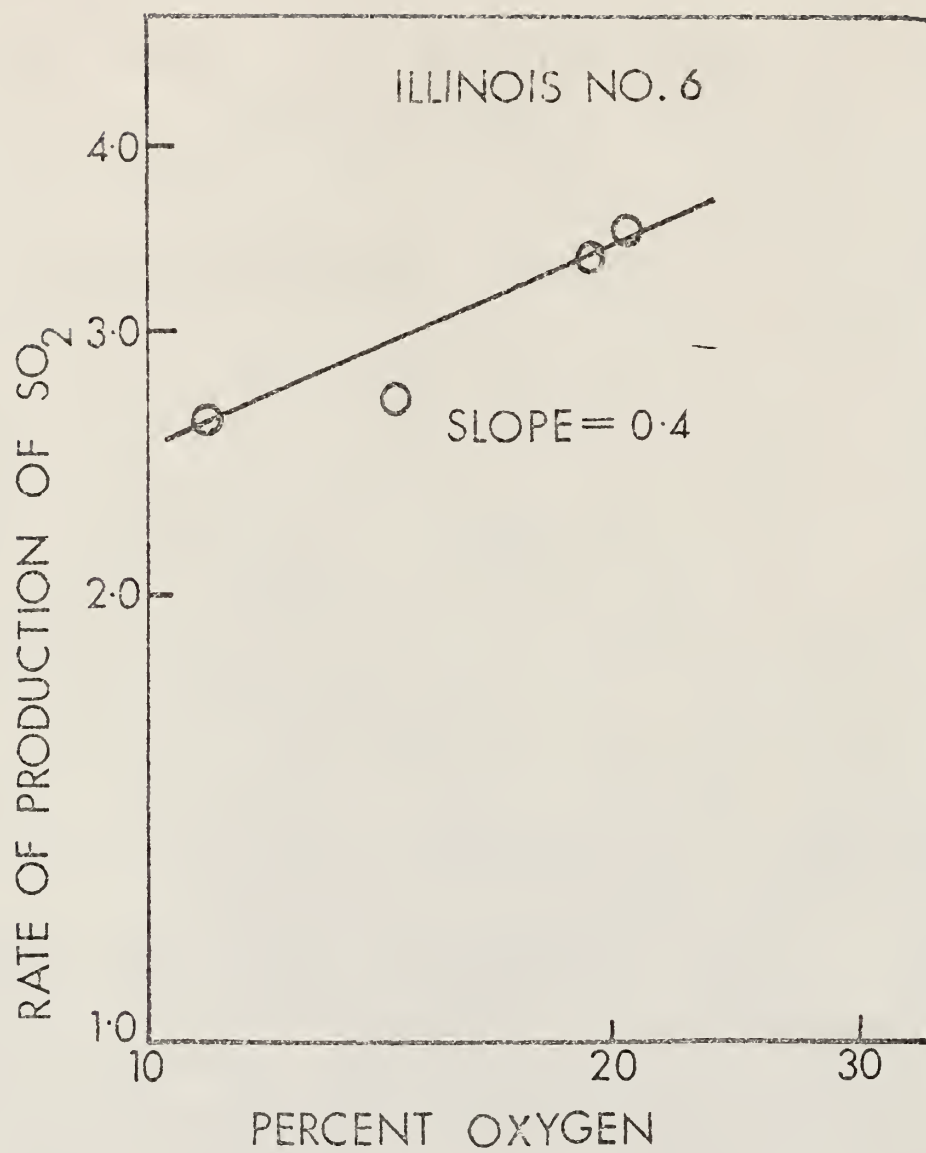
$$\exp \left[\frac{-E}{R} \left(\frac{1}{2400} - \frac{1}{2250}\right)\right] \tag{29}$$

just due to the temperature increase itself. From the activation energies obtained for Illinois No. 6, this factor was found to be about 1.7, and the true reaction order was thus reduced to about 0.175.

Thus the activation energies obtained for the three types of coal are in agreement with the activation energies measured from surface oxidation rates Seeker (2) and secondly the reaction order from both the surface oxidation rates and the rate of production of SO_2 with respect to partial pressure of oxygen are the same. So we can conclude that the overall oxidation of coal governs the emission of SO_2. This is in contrast to the view expressed in the literature. It has been assumed that SO_2 production from coal would be the same as the production of SO_2 from sulfur containing compounds (13,20).

Table 13.   Rate of Production of SO_2 in Coal

Sample	Percentage of Oxygen	Concentration of SO_2 (ppm)	Δt μs	Rate of Production of SO_2 (ppm/μs)
Ill. No. 6	10.10	341.5	1300	0.2626
Ill. No. 6	14.7	498.05	1800	0.2766
Ill. No. 6	20.0	660.00	1900	0.338
Ill. No. 6	21.0	710.00	2000	0.355

Table 14.   Rate of Production of SO_2 in Model Compound

Sample	Percentage of Oxygen	Concentration of SO_2 (ppm)	Δt μs	Rate of Production of SO_2 (ppm/μs)
Thianthrene	10.10	1025.50	1600	0.6409
Thianthrene	14.17	1500.30	1700	0.8825
Thianthrene	20.0	1900.25	1400	1.357
Thianthrene	21.0	2100.65	1425	1.474

5.0   Summary and Recommendations for Further Study

A study of H_2S and SO_2 emissions from fuel bound sulfur in coal
and certain sulfur containing model compounds has been conducted.

The thermal decomposition of the model organic compounds and the
three coals was investigated in the temperature range, 900 K to 1700 K.
The yield of H_2S increased from 900 K to 1470 K and then remained constant
to 1520 K.   Above 1520 K, the yield of H_2S decreased rapidly with in-
creasing temperature.   Assuming first-order kinetics and Arrhenius be-
havior the activation energies for both coal and model compounds were
calculated.   The activation energies for the model compounds were found
to be in good agreement with the literature values.   The activation
energies for coals were in close agreement with the activation energies
obtained for the model compounds.   This suggests that the yields of H_2S
from the organic compounds and the coal were due to the same chemical
reactions.

The two organic model compounds, iron pyrites (Fe_2S) and three
coals were oxidized in air over the temperature range, 900 K to 1850 K.
The yield of SO_2, determined spectrophotometrically, increased with in-
creasing temperature up to 1820 K and was independent of temperature
over 1820 K.   Assuming first-order kinetics and Arrhenius behavior the
activation energies for the coals and the model compounds were calculated.
This is the first reported work on the high-temperature oxidation of the
model compounds in gas phase.   The activation energies were found to be
in reasonable agreement with the literature values for model compounds.

The activation energies for coals were determined and found to be in
close agreement with the activation energies calculated from surface
oxidation rates and also the reaction order from both the surface
oxidation rates and the rate of production of SO_2 with respect to partial
pressure of oxygen are the same. This suggests that the overall oxidation
of coal governs the emission of SO_2; whereas the chemical reactions in-
volving the sulfur bond governed the production of SO_2 in model compounds.

It is recommended that this work be continued with some modifications,
such as mixing coal with calcium carbonate and magnesium carbonate and
studying the SO_2 and H_2S emissions with respect to temperature. Also,
it is recommended to perform the NO_x emission studies from pulverized
coal and model compounds, in order to have a complete knowledge of
emission phenomena of the major pollutants of coal.

Literature Cited

1. Arthur Levy, Earl L. Merryman, and William T. Reid, Environmental Science and Technology, 4, 653 (1970).

2. W. R. Seeker, "The Kinetics of Ignition and Particle Burnout of Coal Dust Suspensions Under Rapid Heating Conditions," Ph.D. Dissertation, Kansas State University, 1979.

3. J. Hall and J. Herrin, "Reaction Rate Determination and Correction for Finite Quenching Rate in Shock Induced Pyrolysis of Methane Via a Simple Shock Tube," ASME 76-GT-13, 1976.

4. D. C. Wegener, "The Production of Lower Molecular Weight Hydrocarbons During the Thermal Decomposition of Pulverized Coal in Air and Nitrogen," M. S. Thesis, Kansas State University, 1978.

5. A. G. Gaydon and I. R. Hurle, The Shock Tube in High Temperature Chemical Physics, (Reinhold, New York, 1963).

6. L. Horton and R. B. Randall, Fuel, 26, 127 (1947).

7. J. K. Chowdary, et al., J. Sci. Ind. Res., 11B, 150 (1952).

8. R. V. Wheeler, Givard, 121, 1596 (1921).

9. J. W. Mellor, Comprehensive Treatise on Theoretical and Inorganic Chemistry, (Longmans, Green and Co., London, 1935), Vol. 14, p. 199.

10. G. M. Schwas, and J. Philinis, J. Am. Chem. Soc., 69, 2588 (1947).

11. C. M. Sulter, Organic Chemistry of Sulfur, (John Wiley and Sons, New York, 1944).

12. E. Emmett Reid, Organic Chemistry of Divalent Sulfur, (Chemical Publg. Co., New York, 1956), 2nd ed.

13. A. Attar and F. Dupuis, Paper Presented to ACS Meeting, Anaheim, Calif., 1974.

14. E. H. Braye, A. H. Sehon, and B. De B. Darwent, J. Am. Chem. Soc., 77, 5282 (1954).

15. A. C. Harkness, and F. E. Murray, Int. J. Air and Water Pollut., 10, 245 (1966).

16. A. H. Sehon, and B. De B. Darwent, J. Am. Chem. Soc., 76, 4806 (1955).

17. A. Attar and William H. Corcoran, Ind. Eng. Chem. Prod. Res. Dev., 16, 2 (1977).

18. A. Attar, Fuel, 57, 201 (1978).

19. W. Fuches, Buesk Chem., 32, 274 (1951).

20. P. H. Given and W. F. Wyss, BCURA, 25, 5 (1961).

21. Amer. Soc. for Testing and Materials Annual Book of Standards, 19, 17 (1973).

22. Amer. Soc. for Testing and Materials Annual Book of Standards, 19, (1974).

23. R. A. Mott, and H. C. Wilkinson, Fuel, 35, 6 (1956).

24. A. Attar and F. Dupuis, Pre. Div. Fuel Chem., ACS, 44, 23 (1978).

25. E. M. Suuberg, W. A. Peters, and J. B. Howard, Ind. Eng. Chem. Process Des. Dev., 17, 1 (1978).

26. L. Bateman and K. B. Hargrave, Proc. Roy Soc. London Ser. A, 224, 339 (1974).

27. M. A. Dankleff, R. Curci, J. O. Edwards, Pyum, Hai-yung, J. Am. Chem. Soc., 90, 3209 (1968).

28. Intersociety Committee, Methods of Air Sampling and Analysis,
     (American Health Assoc. Publg., Washington, D. C., 1968), p. 447-490.

29. P. W. West and G. C. Gaeke, Anal. Chem., 28, 1816 (1956).

30. M. B. Jacobs, M. M. Braverman, and S. Hochheiser, Anal. Chem., 29,
     1349 (1957).

31. M. A. Nettleton, and R. Stirling, Proc. Roy. Soc., A300, 62 (1967).

32. E. Tschuikow-Roux, Phy. of Fluids, 8, 821 (1965).

ACKNOWLEDGEMENTS

I am highly indebted to Dr. J. F. Merklin for his guidance and help during all phases of this work, and especially for his encouragement and advice during my entire stay at Kansas State University.

A special expression of gratitude is extended to Dr. T. W. Lester for his helpful advice and discussions.

Grateful recognition is expressed to Steve Vaughn and Dr. W. R. Seeker for their discussions and suggestions.

I am thankful to the Department of Nuclear Engineering, which provided the financial support. The importance of the typist, Shelly Kemnitz, in the preparation of this manuscript cannot be overstated.

Finally, I thank my Uncle and Aunt, Mr. and Mrs. T. K. Tummala for their love and encouragement.

APPENDIX A

Details of Wet Chemical Procedures

Measurement of Sulfur Dioxide (28)

Reagents: All chemicals used were ACS Analytical Reagent Grade.

Absorbing reagent: 0.04 M Potassium Tetrachloromercurate (TCM).

The absorbing solution is prepared by dissolving 10.86 gm of
mercuric chloride and 5.96 gm of potassium chloride and 0.066 gm of
EDTA in water and diluting to 1 liter of solution.

Sulfamic acid (0.6 percent solution): dissolve 0.6 gm of sulfamic
acid in 100 ml of distilled water.

Pararosaniline (0.2 percent stock solution): dissolve 0.20 gm of
pararosaniline by shaking with 100 ml of 1 N HCL.

Pararosaniline reagent: This was prepared by adding 20 ml of the stock
pararosaniline solution to 250 ml flask and adding 25 ml of 3M H_3PO_4
(phosphoric acid) and diluting to the volume with distilled water.

Formaldehyde (0.2 percent): dilute 5 ml of 40 percent formaldehyde
to a liter with distilled water.

Reagents for standardization:

Stock Iodine solution (0.1 N): add 12.7 gm of Iodine and 40 gm of
potassium iodide to 25 ml of water and keep stirring until dissolved
and then dilute to one liter with distilled water.

Starch Indicator solution: to a mixture of 0.4 gm of soluble starch
and 0.002 gm of mercuric iodide add little water and make it in a paste
and add this to a 200 ml boiling water.

Standard 0.1 N Sodium Thiosulfate Solution: dissolve 25 gm of sodium thiosulfate and 0.1 gm of sodium carbonate and dilute to one liter. Before standardization stand for at least one day. To standarize, weigh 1.5 gm of potassium iodate and dilute to volume in a 500-ml volumetric flask. To a 500-ml iodine flask, pipet 50 ml of the iodate solution. Add 2 gm of potassium iodide and 10 ml of a 1:10 dilution of concentrated hydrochloric acid. Stopper the flask. After 5 min. titrate with thiosulfate to a pale yellow color. Add 5 ml of starch indicator solution and complete the titration.

Normality of thiosulfate

$$= \frac{\text{wt. (gm of } KIO_3) \times 10^3 \times 0.1}{\text{ml of titer} \times 35.67}$$

Standard sulfite solution: dissolve 0.300 gm of Sodium metabisulfite in a 500 ml of distilled water. The actual concentration of the standard solution is determined by adding excess Iodine and back-titrating with sodium thiosulfate.

Back titration: This is performed by accurately pipeting 50 ml of 0.01 N Iodine into two 500 ml flasks. To a flask A (blank) add 25 ml of distilled water and to flask B (sample) pipet 25 ml of the standard sulfite solution. Allow the flasks to stand for 5 minutes to react and then titrate each flask with 0.01 N thiosulfate until they turn pale yellow color. Then add 5 ml of starch solution and continue the titration to the disappearance of the blue color. Calculate the concentration of sulfur dioxide in the standard solution as follows:

$$SO_2 \ \mu g/ml = \frac{(A-B) \ NK}{V}$$

where

A = number of ml for blank

B = number of ml for sample

N = normality of thiosulfate solution

K = microequivalent weight for SO_2 is 32,000

V = sample volume taken.

This sample sulfite solution is diluted by pipeting accurately 2 ml of standard sulfite solution into 100 ml flask and diluting with 0.04 M TCM.

Calibration and Standards: Into 25 ml sampling bottle pipet accurately graduated amounts of dilute sulfite solution (such as 0,1,2,3,4,5 ml) add 0.04 TCM solution to each sampling bottle to bring the volume of its contents to 10 ml. Add 1 ml of sulfamic acid solution, allow it to react for 30-40 minutes. Add 2 ml of 0.6 percent formaldehyde and 5 ml pararosaniline reagent and allow the solution to react for 30 minutes. After 30 minutes, bring all the sampling bottles to the volume with distilled water. After 30 minutes determine the absorbance of the solution and of the blank at 548 nm. The total absorbance of the solution is plotted against the total micrograms of SO_2. From the slope of the plot we can find the calibration factor B (reciprocal of the slope of the line).

Procedure: collection of sample: place 10 ml of 0.04 M TCM solution in a 25 ml sampling bottle and inject (10 or 20 ml) of the sample gas into the 10 ml of absorbing solution. Allow it to react for at least 15-30

minutes. After that add 1 ml of sulfamic acid. Allow it to react for 30-40 minutes and then add 2 ml of formaldehyde and 5 ml of pararosaniline reagent. After 30 minutes bring the bottles to the volume by distilled water and let it stand for 30 minutes. Determine the absorbance of the sample and of the blank at 548 nm.

Calculations: concentration of SO_2 in the sample is computed by the following formula

$$ppm = \frac{(A - Ao)\ 0.382\ B}{V}$$

where

 A = sample absorbance

 Ao = reagent blank absorbance

 0.382 is the volume (ml) of 1 mg of SO_2 at 25 °C and 760 torr

 B = calibration factor (µg/absorbance units)

 V = sample volume in liters

Measurement of Hydrogen Sulfide (28)

Reagents: All chemicals used were ACS analytical reagent grade.

Absorbing Solution: dissolve 4.3 gm of cadmium sulfate and 0.3 gm of sodium hydroxide in separate portions of water, mix, add 10 gm of Arabinogalactan and dilute to 1 liter. Shake the resultant suspension vigorously before removing each aliquot.

Amine-sulfuric acid stock solution: Add 50 ml concentrated sulfuric acid to 30 ml water and cool. Dissolve 12 gm of N, N-dimenthyl-p-phenylenediamine dihydrochloride in the acid.

Amine Test Solution: dilute 25 ml of the stock solution to 1 litre with 1:1 sulfuric acid.

Ferric Chloride Solution: Dissolve 100 gm of ferric chloride in water and dilute to 100 ml.

Ammonium phosphate solution: 400 gm of diammonium phosphate is dissolved in water and diluted to 1 liter.

Standardization and Calibration: Dissolve 0.71 gm of sodium sulfide ($Na_2S . 9 H_2O$) in 1 liter of water, standardize and adjust in the usual manner with standard iodine and thiosulfate solution as used in the previous method for SO_2. Dilute 10 ml of standard sulfide solution to 1 liter for the stock solution.

Ten ml of the absorbing solution is added to a series of 25 ml sampling bottles and then 0,1,2,3, etc. ml of stock sulfide solution is added. The amine-test solution (1.5 ml) is added to each of these bottles and mixed. Then 1 drop of ferric chloride solution is added. Mix and then dilute to volume by adding distilled water and allow to stand for 30 minutes. The absorbance is determined at 670 nm against a sulfide-free reference solution. Then prepare the standard curve of absorbance vs µg H_2S/ml.

Collection of the Sample and Analysis: Place 10 ml of absorbing solution in a 25 ml sample bottle and inject (10 or 20 ml) of the sample gas into the 10 ml of absorbing solution. Allow it to react for at least 30 minutes to one hour. Then add 1.5 ml of amine-test solution and add 1 drop of ferric chloride solution, if SO_2 concentration is higher, add more of ferric chloride and then remove the color due ferric ion by adding 1 drop of ammonium phosphate solution. Continue the addition

of ammonium phosphate solution drop wise until the solution is decolourized.

Make up the solution up to the volume and allow it to stand for 30 minutes.

In the same way prepare a zero reference, i.e., without any gas sample

injected into 10 ml of absorbing solution. Measure the absorbance of

the colour at 670 nm in a spectrophotometer.

Calculations:

$$H_2S \ \mu g/m^3 = \frac{(\mu g \text{ of } H_2S \text{ from the standard curve}) \ 10^3}{V},$$

where

$$V = \text{sample volume,}$$

$$
\begin{array}{ccc}
\text{Concentration} & & \text{Concentration} \\
\text{in } \mu g/m^3 & = & \text{in ppm}
\end{array}
\quad X \ \frac{M}{24,500} \ X \ 10^6
$$

where

M = molecular weight of H_2S

$$ppm = \frac{\mu g/m^3 \ X \ 24,500}{M \ X \ 10^6}$$

APPENDIX B

Details of Total Sulfur Determination (22):

Eschka Method:

Reagents: All chemicals used were ACS Analytical Reagent Grade.

Barium Chloride Solution (100 gm/litre): dissolve 100 gm of barium

chloride in 1 liter of water.

Bromine Water (saturated): add an excess of bromine to 1 liter of water.

Eschka Mixture: thoroughly mix 2 parts by weight of light calcined

magnesium oxide and 1 part of anhydrous sodium carbonate. Both materials

should be as free as possible from sulfur.

Hydrochloric acid (1+1): Mix equal volumes of concentrated hydrochloric

acid (Hcl sp gr 1.19) and water.

Hydrochloric acid (1+9): Mix 1 volume of concentrated hydrochloric acid

(Hcl sp gr 1.19) with 9 volumes of water.

Methyl orange indicator solution (0.2 gm/litre): Dissolve 0.02 gm of

methyl orange in 100 ml of hot water and filter. Sodium carbonate, saturated

solution: dissolve 60 gm of sodium carbonate in 100 ml of water. Sodium

hydroxide solution (110 gm/litre): dissolve 100 gm of sodium hydroxide in

1 litre of water.

Procedure:

Preparation of sample and mixture: Thoroughly mix on glazed paper approxi-

mately 1 gm of the sample (coal) and 3 gm of Eschka mixture. The amount

of sample to be taken will depend on the amount of $BaCl_2$ solution. Trans-

fer this mixture into a porcelain capsule or procelain crucible.

Ignition: place the crucible in a cold muffle and gradually raise
the temperature to 800 ± 25 C in about 1 hour. Maintain this maximum
temperature for about 1 1/2 hours.

Subsequent Treatment: remove the crucible and empty the contents into
a 200 ml beaker and digest with 100 ml of hot water for 30-40 min,
while stirring occasionally. Filter and wash the insoluble residue
with water. Treat the filtrate, amounting to about 250 ml with 10 to
20 ml of saturated bromine water, make slightly acid with HCl, and boil
to expel the liberated bromine. Make just neutral to methyl orange
with NaOH solution; then add 1 ml of HCl (1+9). Boil again and add
slowly 10 ml of $BaCl_2$ solution. The $BaCl_2$ solution must be in excess.
Continue boiling for 15 minutes and allow to stand for at least two
hours. Filter through an ashless paper with hot water until silver
nitrate shows no precipitate with a drop of the filtrate.

Place the wet filter containing the precipitate of barium sulfate in
a weighted platinum, or silica crusible, allowing a free access of air
by folding the paper over the precipitate loosely to prevent spattering.
Smoke the paper off gradually and at no time allow it to burn with flame.
After the paper is consumed, raise the temperature to 925°C and heat to
constant weight.

Dissolve the residue of magnesium oxide, etc. after leaching, in HCl
and test for sulfur. When an appreciable amount is found, this should be
determined quantitatively.

Blanks and Corrections: In all cases, a correction must be applied by running a blank exactly as described above, using the same amount of all reagents that were employed in the regular determination.

Calculations: Calculate the sulfur content as follows:

$S_\% = (A - B) \times 13.738 /C$

A = grams of $BaSO_4$ precipitated

B = grams of $BaSO_4$ in the blank

C = grams of $BaSO_4$ in the sample used.

Bomb washing method:

The bomb washing method is convenient for labs that make frequent coal calorimetric determinations. The bomb is filled with a pressure of 20 atmospheres or at least 5 grams of oxygen per gram coal. The bomb shall stand in the calorimeter water for not less than 5 minutes after firing. Then remove the bomb from the calorimeter water and open the valve carefully so as to allow the gases to escape at an approximately even rate in order that pressure is reduced to atmospheric in not less than one minute. After the combustion is complete, carefully wash all parts of the interior of the bomb with a jet of distilled water containing 1 c.c. per liter of a saturated solution of methyl orange, until no acid reaction is observed. Collect the washing and repeat the procedure as in the case of Eschka procedure.

High temperature combustion method:

In this method a weighed amount of coal sample is burned in a tube furnance in a stream of oxygen at a temperature of 1350 C. The sulfur oxides and chlorine formed are absorbed in H_2O_2 solution yielding HCl and

H_2SO_4. The total acid content is determined by titration with HaOH, and
the amount of NaCl resulting from the titration of the HCl is converted to
NaOH with solution of mercuric oxycayanide $Hg(OH)CN$. This NaOH is de-
termined titrimetrically and used to correct the sulfur value, which is
equivalent to the amount of H_2SO_4 formed during coal combustion. The
reactions taking place are as follows:

$$SO_2 + H_2O_2 \rightarrow H_2SO_4$$

$$Cl_2 + H_2O_2 \rightarrow 2HCl + O_2 \, ,$$

$$NaCl + Hg(OH)CN \rightarrow HgClCN + HaOH \, .$$
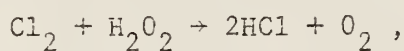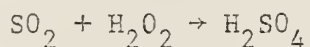
This method is accurate for both low and high sulfur concentrations.

Appendix C

Details of Activation Energy Calculations

The kinetic data analysis was conducted on the assumption that the reactions involved are first order in sulfur containing compounds and obey Arrhenius behavior.

According to the first-order kinetics

$$\frac{dx}{dt} = k_{uc} y , \qquad\qquad D.1$$

where x = amount of SO_2 or H_2S concentration produced,

y = concentration obtained from

$y = (x_{maximum} - x_{at\ every\ temperature})$,

$x_{maximum}$ = the maximum concentration of SO_2 or H_2S obtained as the result of oxidation or pyrolysis,

$x_{at\ every\ temperature}$ = the concentration of SO_2 or H_2S at that particular temperature.

k_{uc} = uncorrected rate constant,

t = time.

For this oxidations, the concentration of oxygen is a constant and k becomes a psuedo first order rate constant.

For example, from the Tables of Ill. No. 6 oxidation, at 1200 K, the concentration of SO_2 obtained was 125.03 ppm. This 125.03 ppm is $x_{at\ that\ temp.\ 1200\ K}$ and x_{max} for Ill. No. 6 oxidation was at temperature 1800 K and was 479.30 ppm of SO_2.

y is obtained at that particular temperature 1200 K as

$$y = (x_{max} - x_{at\ that\ temp.\ 1200\ K}),$$
$$= 479.30 - 125.03,$$
$$y = 354.27\ ppm.$$

Taking the natural logarithm of both sides of Eq. (1), then one obtains,

$$\ln \frac{dx}{dt} \frac{1}{y} = \ln k_{uc}. \qquad\qquad D.2$$

Since we assume that the reaction exhibits Arrhenius behavior and we can substitute for k_{uc} in Eq. D2 and obtain,

$$\ln [\frac{1}{y} \frac{dx}{dt}] = \ln A - E_{exp}/RT \qquad\qquad D.3$$

where A = constant

E_{exp} = Activation energy

R = gas constant

T = Temperature.

Thus a plot of $\ln [\frac{1}{y} \frac{dx}{dt}]$ vs $\frac{1}{T}$ (K^{-1}) gives you a straight line with slope (E_{exp}/R) from which we can calculate the activation energies.

Appendix D

Error Analysis:

Because of the many uncertainties associated with coal research, like mass and heat transfer and chemical kinetics, a concise statement of the error associated with combustion measurements is seldom made. Although research associated with the shock tube minimizes some errors, but others are introduced.

For instance, error is introduced in calculating the reaction zone temperature from the frozen gas equations. It was discussed by Nettleton (31), who predicted errors up to 50 $^\circ$K and by Gaydon and Hurle (5) who reported error up to 25 $^\circ$K to be common for shock tube experimentation.

The uncertainty in the SO_2 of H_2S gas yield had several sources. For instance, inaccuracies in sample dilution multiplication factor, errors in standardization of the wet chemical methods, and the uncertainty in the mass of the initial coal sample. By firing an oxidation shock prior to every sample run, thus the H_2S or SO_2 background is at a minimum and fairly constant level. The greatest errors in SO_2 or H_2S yields was associated in determining the sample dilution multiplication factor (SDMF) at high temperature where mixing between the driver and test gas was extensive. At lower temperatures the error was less than 2% where as at high temperature the error was 10-15%. A source of error is associated with the wet chemical methods. These methods involve elaborate procedures such as weighing samples, making solutions, preparing standards, calib-

rating, etc. During these, many errors are introduced. These errors were minimized as far as possible by doing calibration of the standards two or three times. The results were in close agreement.

Therefore, the errors in SO_2 or H_2S yields may be of the order of 10-20% at the lowest and highest temperature regions, whereas the errors is lower in the intermediate temperature regions. The data obtained were remarkably reproducible. In replication runs, the data agreed to within $\pm$ 5%.

EVOLUTION OF H_2S AND SO_2 DURING RAPID HEATING
OF PULVERIZED COAL AND SULFUR CONTAINING MODEL COMPOUNDS

by

JAYARAM POLAVARAPU

M.Sc., Andhra University, Waltair, India, 1975

AN ABSTRACT OF A MASTER'S THESIS

submitted in partial fulfillment of the
requirements for the degree

MASTER OF SCIENCE

Department of Nuclear Engineering
KANSAS STATE UNIVERSITY
Manhattan, Kansas

1979

Abstract

A study of H_2S and SO_2 emissions from fuel bound sulfur in coal
has been conducted. Pittsburgh Seam, Illinois #6, and Mo-Kan coals
were studied and compared to three model compounds. The three model
sulfur compounds were iron-pyrites (FeS_2), thianthrene [$(C_6H_4S)_2$ -
aromatic sulfur], and L-cystine [$(-SCH_2CH(NH_2)COOH)_2$ - aliphatic
sulfur].

The thermal decomposition of the model organic compounds and the
three coals was investigated in the temperature range, 900 K to 1700 K,
using the chemical shock tube. The yield of H_2S increased from 900 K
to 1470 K and then remained constant to 1520 K. Above 1520 K, the
yield of H_2S decreased rapidly with increasing temperature. The kinetic
analysis of the data gave an activation energies of 52 kcal/mole for
L-cystine and 55 kcal/mole for Thianthrene. For the coals the activation
energies obtained are 50 kcal/mole for Pittsburgh Seam, 54 kcal/mole
for Illinois #6, and 50 kcal/mole for Mo-Kan. Thus, the kinetic
analysis of the yields of H_2S from the organic model compounds and the
coals indicated that the chemical reactions leading to the formation of
H_2S were the same in all cases.

The two organic model compounds, iron-pyrites (FeS_2) and three
coals were oxidized in air over the temperature range, 1175 K to 2200 K.
The yield of SO_2 increased with increasing temperature up to 2100 K and
was independent of temperature above 2100 K. The yield at this point
corresponds to 100% conversion of sulfur to SO_2 in the three coals.

Kinetic analysis of the data gave an activation energies of 10 kcal/ mole for iron-pyrites, 19 kcal/mole for L-cystine and 20 kcal/mole for Thainthrene. For the coals we have an activation energies of 38 kcal/mole for Pittsburgh Seam, 40 kcal/mole for Illinois #6, and 39 kcal/mole for Mo-Kan. From these kinetic analysis of the temperature dependence of the SO_2 yields from iron pyrites and the model organic compounds indicated that similar chemical reactions, involving the sulfur bond, governed the production of SO_2. In contrast kinetic analysis of the SO_2 yields from the three coals indicated that the overall oxidation of coal governed the emission of SO_2.